THE UNIVERSITY OF MANITOBA

FREE CONVECTION FROM A VERTICAL PLATE TO WATER NEAR $4^{o}C$

by

M. P. Hasinoff

A Thesis

Submitted to the Faculty of Graduate Studies

in Partial Fulfilment of the Requirements for the Degree

of Master of Science

Department of Mechanical Engineering

Winnipeg, Manitoba

May, 1976

"FREE CONVECTION
FROM A VERTICAL PLATE TO
WATER NEAR 4°C"

by

M. P. Hasinoff

A dissertation submitted to the Faculty of Graduate Studies of the University of Manitoba in partial fulfillment of the requirements of the degree of

MASTER OF SCIENCE

ABSTRACT

This thesis is an experimental investigation of the free convection heat transfer process from a vertical isothermal plate to water at temperatures below $4^{o}C$, the temperature of the maximum density of water.

Earlier researchers have defined the boundaries of the different flow regions in terms of plate and bulk temperatures. The regions in which unidirectional flow exists have been throughly investigated analytically and experimentally. However, in the region in which bidirectional flow exists an exact theoretical analysis was not available. A number of researchers have made experimental measurements in this region and experimental correlations for the local heat flux are available. The nature of the flow has been investigated and researchers have postulated that certain flow patterns exist.

Initial tests in the present investigation were conducted in a region in which purely downward flow was known to exist. Experimental measurements were recorded and the mean experimental heat transfer coefficients were compared with theoretical predictions obtained using equations developed in an earlier investigation. The results gave an indication of the accuracy

of the experimental apparatus.

The balance of the tests were conducted in the bidirectional flow region. Mean experimental heat transfer coefficients were evaluated and compared with predictions from an earlier experimental correlation. The results of the comparison suggest that a further refinement of the correlation is necessary.

The bidirectional flow patterns were examined using the "thymol blue" flow visualization technique. Neutrally bouyant dye is produced in the region of interest and the dye traces out the flow patterns. The flow visualization studies confirmed the existence of two types of bidirectional flow. In "separated" bidirectional flow the inner upward flowing boundary layer separates from the plate and reverses its direction at the top of the heated section to flow into the outer downward flowing boundary layer. In "non-separated" bidirectional flow the inner upward flowing boundary layer continues flowing up past the top of the heated section and does not separate from the plate.

ACKNOWLEDGEMENTS

I would like to express my sincere thanks to the many individuals who have assisted me in this work. I would like to thank my advisor, Dr. G. K. Yuill, for his guidance, encouragement, criticisms, and suggestions. Thanks are also due my fellow graduate students whose many suggestions have been invaluable. I would like to thank Mr. L. W. Wilkins for his assistance in the construction of the apparatus, Mr. D. Schaldemose for his suggestions on the electrical circuitry, and Mrs. Denise Morrison for her careful typing of this thesis.

I am grateful to the Water Research Office of the Inland Waters Directorate of Environment Canada for the financial assistance that made my studies possible.

I would also like to thank my parents for their continued encouragement. Most important of all I would like to thank my wife, Suzanne, whose patience, encouragement, and love have helped me to complete this work.

TABLE OF CONTENTS

	Page
ABSTRACT	i
ACKNOWLEDGEMENTS	iii
TABLE OF CONTENTS	iv
LIST OF FIGURES	vii
LIST OF TABLES	viii
NOMENCLATURE	ix
CHAPTER 1 INTRODUCTION	1
1.1 The Problem	1
1.2 The Phenomenon	3
1.3 Previous Work	6
1.3.1 Free Convection	6
1.3.2 Free Convection in Water Near $4^{o}C$	6
CHAPTER 2 EXPERIMENTAL STUDY	22
2.1 The Objectives	22
2.2 Experimental Apparatus	25
2.2.1 The Plate	25
2.2.2 The Heater Controls and Circuitry	31
2.2.3 Temperature and Voltage Drop Measurement	35
2.2.4 The Tank	38
2.2.5 The Cold Room	39
2.2.6 The Flow Visualization Technique	39

Page

2.2.7 The Plate Support and Dye-Producing Probe 40

2.2.8 Miscellaneous Equipment and Apparatus 42

2.3 Experimental Procedure 44

2.3.1 Heat Transfer Measurements 44

2.3.2 Flow Visualization Technique 49

CHAPTER 3 ANALYSIS OF RESULTS 52

3.1 Heat Transfer Results 52

3.1.1 Distribution of Results 52

3.1.2 Data Processing 52

3.1.3 Examination of Results in Region I and Comparison with Yuill's Theoretical Model 56

3.1.4 Examination of Results in the Region of Bidirectional Flow and Comparison with Yuill's Correlations 59

3.2 Flow Visualization Results 69

3.2.1 Distribution of Results 69

3.2.2 Examination of Flow Patterns 72

3.2.3 Boundary Layer Measurements 83

3.2.4 Comparison of Results with Yuill's Hypothesis 87

CHAPTER 4 CONCLUSIONS 89

REFERENCES 91

Page

APPENDICES

APPENDIX I	VARIATION OF HEATER RESISTANCE WITH TEMPERATURE	94
APPENDIX II	DECAY OF TEMPERATURE ALONG THE ADIABATIC SECTION	96

LIST OF FIGURES

		Page
1.	Map of Free Convection Zones in Low Temperature Water	4
2.	Coefficient C_I vs α in Region I	15
3.	Coefficient C_{III} vs ϕ in Regions III and IV	15
4.	Plate Dimensions	26
5.	Thermocouple Locations	28
6.	Schematic of Main and Guard Heater Circuits	32
7.	Control Turret	34
8.	Plate Support and Dye Producing Probe	41
9.	Location of Experiments	53
10.	Per Cent Error vs ϕ	65
11.	Per Cent Error vs γ	66
12.	Flow Visualization Test Locations	70
13.	Test 15.1 Flow Visualization Photographs	74

LIST OF TABLES

In Text		Page
I	DEVIATIONS FROM AN ISOTHERMAL PLATE	54
II	COMPARISON OF EXPERIMENTAL AND ANALYTICAL HEAT TRANSFER RESULTS IN REGION I	58
III	COMPARISON OF EXPERIMENTAL RESULTS AND YUILL'S CORRELATION IN REGION II-S	62
IV	FLOW VISUALIZATION TESTS	71
V	BOUNDARY LAYER DIMENSIONS	84

In Appendices		
I-A	VARIATION OF HEATER RESISTANCE	95
II-A	COMPARISON OF TEMPERATURE OF LAST HEATED SECTION AND FIRST UNHEATED SECTION	97

NOMENCLATURE

A	Coefficients defined by Equations (1-10), (1-11), (1-14), and (1-15)
B	Coefficients defined by Equations (1-10), (1-11), and (1-15)
C	Coefficient defined by Equations (1-8), (1-11), and (1-16)
C_I	Coefficient defined by Equation (1-10)
C_{III}	Coefficient defined by Equation (1-11)
C_{II-N}	Coefficient defined by Equation (1-14)
C_i	Coefficient defined by Equation (1-15)
C_o	Coefficient defined by Equation (1-16)
D	Coefficient defined by Equations (1-10), (1-11), and (1-16)
E	Coefficient in Equations (1-17) and (1-18)
F	Coefficient in Equation (1-17) and (1-18)
G	Coefficient in Equation (1-10)
Gr	Grashof number
Gr_x	Conventional local Grashof number
Gr'_x	Local Grashof number defined by Equation (1-9)
Gr''_x	Local Grashof number defined by Equation (1-1)
Gr_i	Local inner Grashof number defined by Equation (1-13)

Gr_o	Local outer Grashof number
g	Gravitational acceleration
h	Heat transfer coefficient
k	Thermal conductivity
L	Plate height
m	Exponent defined by Equation (1-18)
Nu	Nusselt number
n	Exponent defined by Equation (1-17)
P	Density function in Equation (1-2)
Pr	Prandtl number
Q	Density function in Equation (1-2)
Ra	Rayleigh number
R_x	Local thermal resistance of the boundary layer
R_T	Electrical resistance of heater at temperature, T
R_5	Electrical resistance of heater at 5^oC
S	Slope of heater resistance versus temperature curve, temperature gradient from last heated to first unheated plate
T	Temperature (^oC)
U	Density function in Equation (1-5)
x	Vertical space coordinate
Z	Coefficient in Equation (1-10)
$\propto$	Bouyancy function defined by Equation (1-2)

β	Thermal expansion coefficient
γ	Angle around the point ($4^{o}C$, $4^{o}C$) on a graph of plate temperature versus fluid temperature as indicated on Figure 1
θ	$T - T_{\infty}$
ν	Kinematic viscosity
ρ	Density
ϕ	Temperature function defined on page 17

SUBSCRIPTS AND SUPERSCRIPTS

(See also the variables to which they are attached in the above list)

b	in the bulk fluid
f	at the film temperature, $(T_p + T_{\infty})/2$
i	of the inner boundary layer
o	of the outer boundary layer
p	at the plate
T	theoretical
x	the local value at position x
I	in Region I
II-N	in Region II-N
III	in Region III
—	average value
'	a non-standard definition
∞	in the bulk fluid

CHAPTER 1

INTRODUCTION

1.1 The Problem

For most fluids density varies linearly with temperature. However, water, antimony, gallium, and bismuth all possess density maxima above their freezing points. For water the maximum density occurs at $4^{o}C$. The significance of this temperature becomes apparent when one considers the enormous amount of water on the earth's surface that seasonally passes through the point of maximum density.

The density maximum of water is not a factor in forced convection unless the velocity is very low as in mixed free and forced convection.

In the analysis of free convection, with density difference the driving force of fluid movement, one must take into account the peculiar behavior of water at $4^{o}C$ and consider the effects it may have on the process.

A great many natural bodies of water pass through the density maximum in the spring and fall. Discharges of heated condenser water from industrial plants, power plants and chemical plants into ice-covered or partially ice-covered bodies of water can disrupt the normal formation of ice. A thermal plume can influence the physical and

biological makeup of a body of water. A knowledge of the behavior of water near $4^{o}C$ is important in furthering the study of the physical processes that take place.

1.2 The Phenomenon

Vanier (2) mapped the free convection process into four regions as shown in Figure 1; a map of plate temperature versus bulk temperature. Yuill (1) has provided a complete description of the processes involved in free convection from a vertical flat plate to water at $0^{o}C$ to $26.8^{o}C$. The process is divided into zones of purely downward flow and purely upward flow and a zone in which there is bidirectional flow.

With the bulk temperature at $0^{o}C$ and the plate temperature between $0^{o}C$ and $4^{o}C$ water adjacent to the plate is heated. Its density exceeds that of the bulk fluid and a net downward flow of fluid results. For plate temperatures between $4^{o}C$ and $8^{o}C$, water within the thermal boundary layer is still denser than the bulk fluid and sinks. At a plate temperature just above $8^{o}C$ the water immediately adjacent to the plate is lighter than the bulk fluid but does not rise; it is pulled downward due to the drag of the outer downward moving thermal boundary layer. The water adjacent to the plate surface has sufficient bouyancy to balance the downward viscous shear force at a plate temperature of about $12.4^{o}C$. This results in a zero velocity gradient at the plate. Between $12.4^{o}C$ and $26.8^{o}C$ the inner upward flowing boundary layer

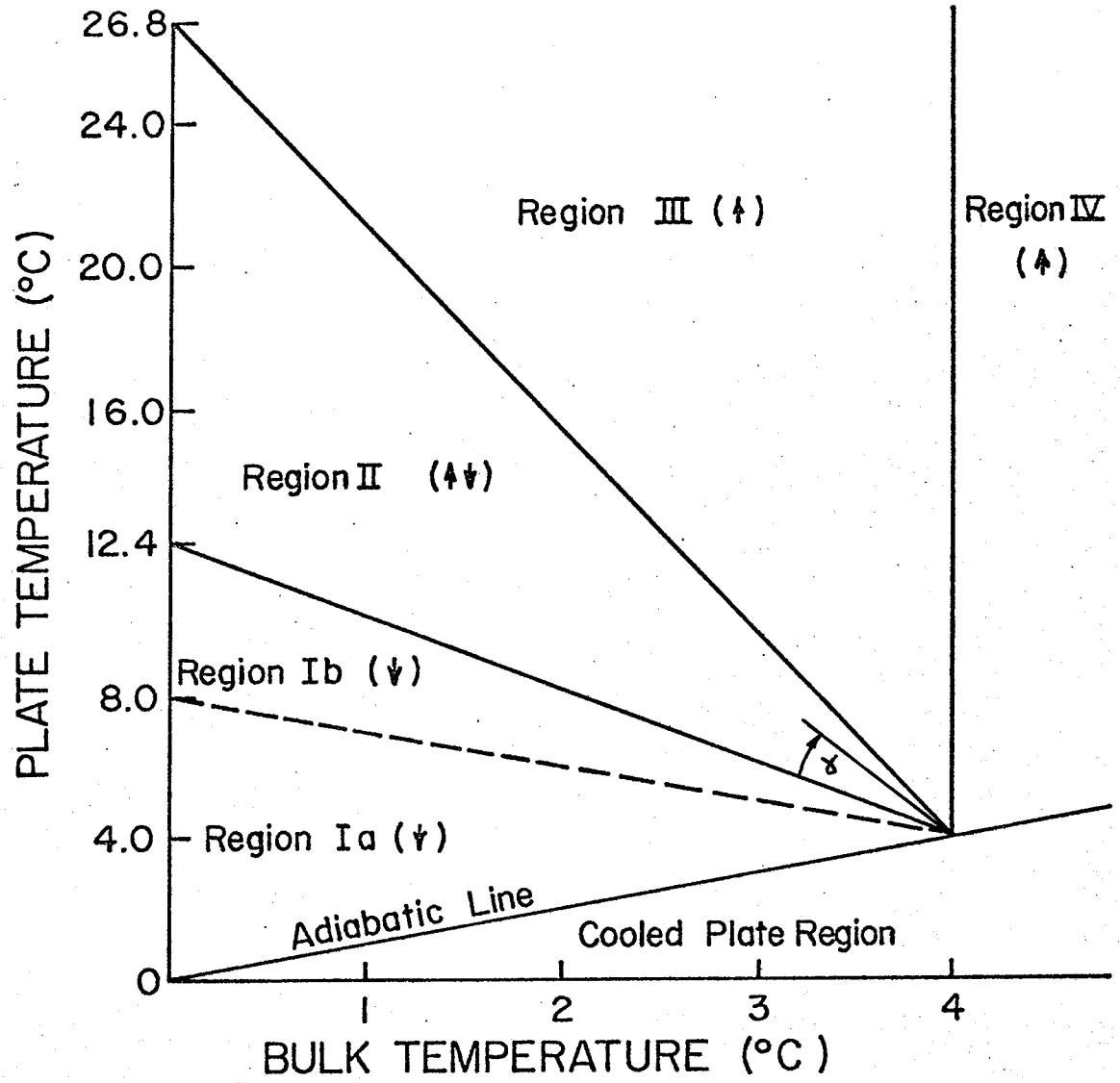

FIGURE 1 MAP OF FREE CONVECTION ZONES IN LOW TEMPERATURE WATER

increases in thickness and bidirectional flow persists. Above 26.8^{o}C the downward motion of the outer boundary layer is stopped by the viscous shear force of the inner layer and unidirectional flow exists. The flow pattern predicted for any combination of plate and bulk temperature is indicated in Figure 1.

1.3 Previous Work

1.3.1 Free Convection

Considerable research has been done in the field of free convective heat transfer since Lorenz (3) first published his analysis of the problem. In 1930 Schmidt and Beckmann applied laminar boundary layer theory to the free convection problem using a series expansion technique (4). Polhausen (5) introduced the similarity transformation technique whereby he transformed the partial differential equations of free convection into ordinary differential equations. Several approximate methods have been proposed since then.

1.3.2 Free Convection in Water Near $4^{o}C$

The first researcher to report the unusual nature of free convection in water near $4^{o}C$ was Codegone (6) in 1939. He found that the rate of heating or cooling a flask of water was at a minimum when the water was at $4^{o}C$.

Ede (7) compiled a study of heat transfer from a vertical plate to several liquids. For all fluids except water the heat transfer rate correlated to the difference between the plate and fluid temperatures. He excluded tests in which the water temperature was below $4^{o}C$ and the plate temperature was above $4^{o}C$ attributing the water

results to the density maximum at $4^{o}C$.

Several authors (8, 9) have reported studies on the melting of ice spheres and horizontal and vertical ice cylinders by the process of free convection in water. They found that at temperatures near $4^{o}C$ a minimum value of the Nusselt number occurred. Tkachev (8) and Dumore, Merk, and Prins (9) performed their studies in 1953. Dumore et al could predict the effect by replacing the conventional thermal expansion coefficient in the empirical free convection equation,

$$Nu = 0.6\ (Pr\ Gr)^{\frac{1}{4}}$$

with a new coefficient that was a linear function of the bulk fluid temperature.

In 1954 Merk (10) applied an integral method to the prediction of melting rates of ice spheres in water. He used a third order polynomial for density as a function of temperature in the boundary layer momentum equation and solved for an infinite Prandtl number. The results were later extrapolated to a Prandtl number of 10. A minimum Nusselt number was predicted to occur at $5.3^{o}C$.

The following year Ede (22) compared Merk's method with the results he had obtained for the heat transfer

from an electrically heated vertical flat plate. For Regions I, III, and IV agreement was good. However, in Region II the predicted Nusselt numbers were as much as 50% low.

In 1956 Schechter and Isbin (12,13) studied the heat transfer from a vertical flat plate to water at a temperature of $4^{o}C$. They applied the similarity transformation introducing Merk's expression for the thermal expansion coefficient into the boundary layer momentum equation. The equations were then transformed into ordinary differential equations using the method of Ostrach (14). The equations were solved, using an analog computer, for the case of plate temperatures from $1^{o}C$ to $14^{o}C$ in a bulk fluid at $0^{o}C$.

They found that the Nusselt number decreased up to a plate temperature of $14^{o}C$. Schechter and Isbin referred to this point as the transition point to bidirectional flow. At these conditions the computed boundary layer velocity profile showed a zero gradient at the plate. Solutions above $14^{o}C$ were not possible as the assumptions used in the similarity transformations are not valid in the bidirection flow region.

They applied the Squire-Eckert integral method to the problem to obtain the equations for the local Nusselt

number;

$$Nu_x = 0.669\ Pr^{\frac{1}{2}}\ (.952 + Pr)^{-\frac{1}{4}}\ (Gr_x''\alpha)^{\frac{1}{4}} \quad \text{.....(1-1)}$$

where $Gr_x'' = g\beta_\infty \theta_p\ x^3/\nu^2$

Schechter and Isbin evaluated the thermal expansion coefficient for Gr_x'' at the bulk temperature instead of the film temperature. The density function α is a dimensionless mean boundary layer density deficit and is defined as:

$$\alpha = 1/3 + P/5 + Q/7 \quad \text{.....(1-2)}$$

where P and Q are density functions defined below:

$$P = (D_2 + 3D_3\ T_\infty)\ /\theta_p\ /\ (D_1 + 2D_2\ T_\infty + 3D_3\ T_\infty^2) \quad \text{.....(1-2a)}$$

and

$$Q = D_3\theta_p^2\ /\ (D_1 + 2D_2\ T_\infty + 3D_3\ T_\infty^2). \quad \text{.....(1-2b)}$$

The constants D_1, D_2, and D_3 are density coefficients and their values were given by Vanier (2) as:

$$D_1 = - 0.6669167 \times 10^{-4} \ C^{-1}$$

$$D_2 = 0.871689 \times 10^{-5} \ C^{-2}$$

$$D_3 = - 0.647664 \times 10^{-7} \ C^{-3}.$$

Schecter (13) also performed experimental measurements of free convective heat transfer from a one foot square vertical heated plate to water below $4^{o}C$. He attempted to measure the velocity and temperature profiles in the boundary layer.

In three of his tests the flow moved up the plate while for seventeen tests downward flow was observed. In ten tests Schechter observed an upward convective flow near the plate and a downward flow further away from the plate surface. Three of the runs were in Region III but

exhibited bidirectional flow. Schechter claimed this was caused either by the effect of limited tank size or temperature conditions that induced a downward flow in the central region of the tank.

Schechter also applied the Squire-Eckert integral method to the bidirectional flow region. He assumed that thermal and momentum boundary layers were equal. He also assumed that all the heat transferred to the inner upward moving boundary layer from the plate returned in the downward flowing boundary layer. By making some further assumptions he obtained the following relations for the local and mean Nusselt number in Region II:

$$Nu_x = 0.489\ [PrGr_x" \propto (x/L\ (U-1) + x)]^{1/4} \quad \ldots\ldots\ldots\ldots (1\text{-}3)$$

$$\text{and}\quad \overline{Nu} = 0.652\ [PrGr_x"]^{1/4}\ (U^{3/4}-1)/(U-1)^{3/4} \quad \ldots\ldots\ldots\ldots (1\text{-}4)$$

$$\text{where}\ U = [30(1/10 + P/14 + Q/18)/\propto]^{4/3} \quad \ldots\ldots\ldots\ldots\ldots\ldots (1\text{-}5)$$

In their paper in 1958 Schechter and Isbin (23) reported a slightly different approximate analysis which yielded the equations:

$$Nu_x = 0.489\ (Gr_x"\ Pr_f \propto)^{1/4} \quad \ldots\ldots\ldots\ldots\ldots\ldots\ldots\ldots (1\text{-}6)$$

$$\overline{Nu} = 0.652 \ (\overline{Gr} \ " \ Pr_f \propto)^{\frac{1}{4}} \quad \ldots\ldots\ldots\ldots\ldots\ldots\ldots\ldots (1\text{-}7)$$

In Schechter's analysis the bulk fluid thermal expansion coefficient approaches zero at $4^{o}C$. Goren (15), in 1966, developed a method of solution that is valid at $4^{o}C$. He introduced into the boundary layer equation a parabolic expression for the density change of water as a function of its temperature deviation from $4^{o}C$. He applied similarity and obtained numerical solutions for free convective heat transfer rates for four different temperature differences from $1^{o}C$ to $0.\overline{001}^{o}C$.

In 1967 Oborin (16) studied free convective heat transfer from a heated sphere and heated cylinder to water in the temperature range from $1^{o}C$ to $15^{o}C$. The sphere was maintained $7^{o}C$ above the water temperature and the cylinder $2.1^{o}C$ above the water temperature. For the sphere the minimum Nusselt number occurred at a water temperature of $2.4^{o}C$ and for the cylinder the minimum occurred at $3.3^{o}C$. He assumed that the minimum heat transfer rate would occur when the mean boundary layer temperature was the same as that of the bulk fluid.

Bidirectional convection was observed by Schenk and

Schenkels (17) in their 1968 study of the melting rates of ice spheres in water. They used a high intensity light to make dust particles in water visible and observed upward flow near the melting surface and downward flow further out when the bulk temperature was between $4^{o}C$ and $6^{o}C$. With the bulk temperature below $4^{o}C$ they observed pure downward convection and when the bulk temperature was above $6^{o}C$ they observed pure upward flow.

They observed a minimum heat transfer rate during melting at $5.3^{o}C$. This was also the temperature predicted by Merk (10) to give the lowest Nusselt number. Above $6^{o}C$ Merk's theory was compatible with Schenk and Schenkels observations but between $4^{o}C$ and $6^{o}C$ great discrepancies were observed. Merk's polynomial could not describe the bidirectional flow present in this temperature range. Below $4^{o}C$ they observed a 20% higher melting rate than was predicted.

Vanier and Tien (2, 18, 19) also studied the melting of ice spheres in water. They found a minimum Nusselt number to occur at $5.35^{o}C$ and they correlated their experimental data as

$$Nu = 2 + C(Ra)^{\frac{1}{4}}.$$

They obtained three values of C, each valid for different bulk temperature ranges.

Vanier and Tien (2, 20, 21) performed a theoretical study of convective heat transfer from a vertical flat plate to cold water. The ordinary differential equations of the boundary layer, obtained by a similarity transformation, were numerically integrated. They considered variable properties by using a Prandtl number that was evaluated at the mean boundary layer temperature. A comparison was made using a Prandtl number appropriate to the local temperature at each step of the numerical integration. They did not find large differences and thus used the mean Prandtl number to save computer time. Solutions in Region II were not possible again as similarity does not apply in the bidirectional flow region. The method described above was used, with modifications, to examine the melting of a vertical flat plate of ice.

The most recent investigation of free convective heat transfer from a vertical flat plate to water near $4^{o}C$ was carried out by Yuill (1). He performed both experimental measurements and theoretical calculations. Theoretical (analytical) solutions were obtained for the regions of unidirectional flow; namely Regions I, III, and IV. A similarity solution of the boundary layer equations

governing free convective heat transfer was used. He included the effect of variable viscosity in the solution. All fluid properties were fitted to polynomial equations. He solved the ordinary differential equations, obtained by a similarity transformation of the partial differential boundary layer equations, using Runge-Kutta forward integration, on a digital computer.

He obtained about 150 solutions in Region I, 260 in Region III, and 120 in Region IV. No solutions were possible for bulk temperatures between 3.3°C and 5.25°C due to a singularity at a bulk temperature of 4°C.

Yuill presented his results in the form traditionally used for the presentation of free convection heat transfer correlations, namely:

$$Nu_x = C(Gr'_x\ Pr)^{1/4}, \quad \text{.....(1-8)}$$

$$\text{where } Gr'_x = 3\alpha\beta\theta_p\ g\ x^3\ /\nu^2, \quad \text{.....(1-9)}$$

and α is defined by Equation (1-2).

The coefficient C was found to correlate well as a function of α in Region I. The relationship is illustrated in Figure 2 with the curve representing the equation:

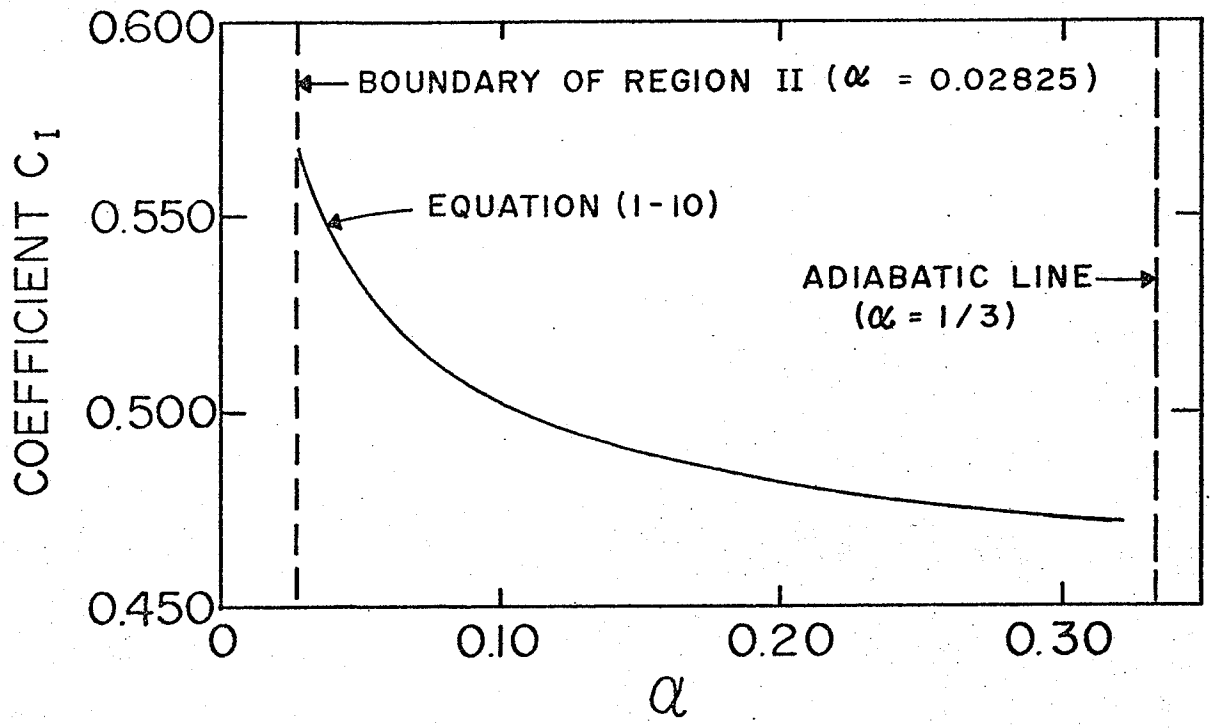

FIGURE 2 COEFFICIENT C_I vs α
IN REGION I

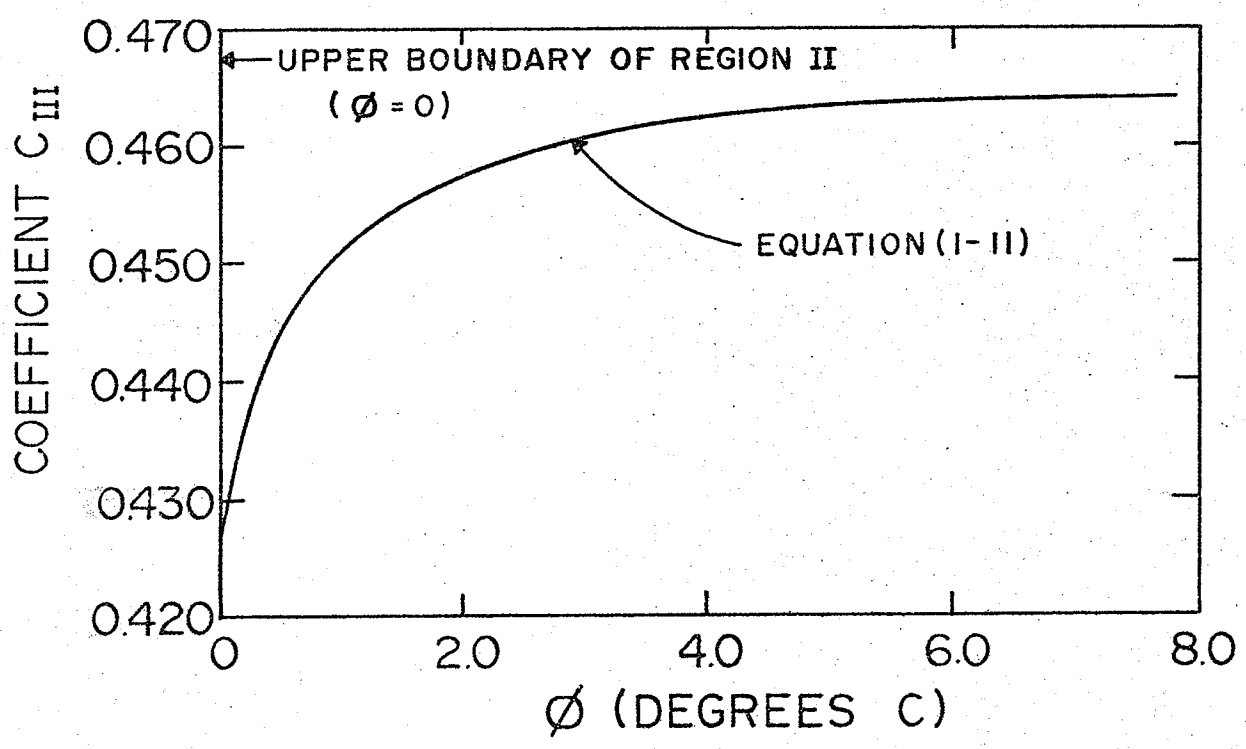

FIGURE 3 COEFFICIENT C_{III} vs ϕ
IN REGIONS III AND IV

$$C_I = -0.568 + 0.098\ (1-\exp(AZ+BZ^2+GZ^3+DZ^4)) \quad \ldots\ldots (1\text{-}10)$$

where $Z = \propto -0.0285$
$A = -23.043$
$B = 130.688$
$G = -469$, and
$D = 406$.

For Regions III and IV the coefficient C_{III} was correlated as a function of the distance from the line $Tp = 4 + 5.7\ (T_\infty - 4)$ which is the boundary between Regions II and III on the plot of plate temperature versus bulk temperature. The distance normal to this line, ϕ , was used to correlate. The results were fitted to the equation:

$$C_{III} = 0.426+0.039(1-\exp(A\phi+B\phi^2+C\phi^3+D\phi^4)) \quad \ldots\ldots (1\text{-}11)$$

where $A = -1.28369\ C^{-1}_{-2}$
$B = 0.321533\ C^{-3}$
$C = -0.0581512\ C_{-4}$, and
$D = 0.00377369\ C^{\ }$.

The curve generated by the equation for C_{III} is shown on Figure 3. Yuill did not obtain results between 3.3°C and 5.25°C.

For Region II no theoretical predictions could be made. Yuill studied the local variation of heat transfer and its dependence on plate height and on distance from the top of the plate and bottom of the plate in the region of bidirectional flow. He measured the local heat fluxes on a vertical isothermal flat plate for several plate lengths and combinations of plate and bulk temperatures in Region II.

Yuill correlated the experimental results by assuming that, in the bidirectional flow region, two boundary layers grow on the plate; an inside layer that grows up the plate and an outside layer that grows down the plate. Investigation of the data led to a further breakdown of the Region II results into regions of "separated" flow and "non-separated" flow. In the "non-separated" flow region, Region II-N, he postulated that the inner boundary layer flowed up past the heated section of the plate insulating the unheated section above from the bulk fluid. In the "separated" flow region, Region II-S, he postulated that the inner upward flowing boundary layer separated from the plate to flow back down as the outer boundary layer.

Arbitrarily he assigned the line $\phi = -.6$ as the boundary between the regions.

In the "non-separated" region Yuill found that the variation of heat flux along the plate was the same as in the regions of unidirectional flow. An equation,

$$Nu_x = C_{II-N} (Gr_i \, Pr_i)^{\frac{1}{4}} \quad \text{.....(1-12)}$$

where $Gr_i = 3\alpha_i g \beta_\infty \theta_p x^3 / \nu_i^2$ .....(1-13)

was used. The quantity α_i is a dimensionless mean boundary layer density deficit for the inner boundary defined by Yuill (1). With the above correlation the coefficient C_{II-N} could be predicted as a simple function of ϕ, the distance from the Region II - Region III boundary. For $\phi = 0$, C_{II-N} was predicted to be .3425. Yuill obtained the equation

$$C_{II-N} = .3425 + A\phi \quad \text{.....(1-14)}$$

where A = 0.080 per degree Celsius. The root - mean - square (rms) deviation of the measured values of C_{II-N} from the equation was 0.02603 or 6.35%.

In the region designated as "separated" bidirectional flow Yuill found that the data could not be easily fit to the equation

$$h = C/x^n .$$

He used a bidirectional model utilizing the concepts of inner and outer boundary layers to evaluate the local thermal resistance of the boundary layer as:

$$R_x = 1/h_{ix} + 1/h_{ox} = C_i (x/k_i)(Gr_i Pr_i)^{-n} + C_o((L-x)/k_o)(Gr_o Pr_o)^{-m} \quad \text{.....(1-14)}$$

The correlating variables were C_i and C_o. A new variable γ, the angle about the point $T_{plate} = 4^oC$ and $T_{bulk} = 4^oC$, was defined and the equations for C_i and C_o were as follows:

$$C_i = 6.988\,\gamma + A\phi\gamma + B\phi\gamma^2 \quad \text{.....(1-15)}$$

and $$C_o = 2.3313 - 8.6188\,\gamma + C\phi\gamma + D\phi\gamma^2 \quad \text{.....(1-16)}$$

The exponents n and m were given as

$$n = .25 + E\phi \quad \text{.....(1-17)}$$

and $$m = .25 + F\gamma \; . \quad \text{.....(1-18)}$$

The values of the coefficients in equations (1-15), (1-16), (1-17) and (1-18) which were obtained from a least squares fit were:

$A = -23.329\ (1/^{o}C)$
$B = 34.907\ (1/^{o}C)$
$C = 6.5212\ (1/^{o}C)$
$D = -19.089\ (1/^{o}C)$
$E = -0.021943\ (1/^{o}C)$, and
$F = -0.051359\ (1/^{o}C)$.

The correlation predicted results at the top and bottom of the plate that were in considerable error. Yuill could not develop a better model or correlation without a better understanding of the actual flow phenomena existing at the plate surface.

CHAPTER 2

EXPERIMENTAL STUDY

2.1 The Objective

In their study of natural convection heat transfer in regions of maximum fluid density Schechter and Isbin (12, 13) observed the bidirectional boundary layer flow along a vertical flat isothermal plate. They introduced neutrally bouyant spheres into the boundary layer to trace out the flow patterns. The flow patterns visualized indicated the presence of bidirectional flow within the boundary layer. The flow was observed to be upward adjacent to the plate and downward farther away from the plate. The study however, was limited and they obtained little conclusive data on the flow patterns or flow velocities.

Yuill (1) studied the local variation of heat transfer from a vertical isothermal plate to water with plate and bulk temperatures in the bidirectional flow region. In his attempt to correlate the data obtained in the bidirectional region he noticed that the data could be further subdivided into two groups depending on the magnitude of the temperature difference between the last heated section and first unheated section of the vertical plate.

For one group the data seemed to indicate that the upward flowing inner boundary layer separated from the plate

and reversed its flow direction to return as the outer boundary layer. For the second group it appeared that the inner upward flowing boundary layer continued flowing upward past the heated section for a distance, insulating the unheated plate from the bulk fluid. The extent or height to which the fluid continued upward could not be accurately determined.

The existence of two regions of bidirectional flow, namely a "separated" flow region and a "non-separated" region could only be postulated because insufficient data had been obtained and no flow visualization studies had been performed. Yuill could not clearly establish the point at which the flow changed from "separated" to "non-separated".

The objectives of the experimental study described below were to further investigate the free convective flows in Region II, the region of bidirectional flow. Attempts were made to duplicate several of Yuill's experimental runs in Region II to obtain more data and also to verify Yuill's test results by using a different apparatus. The existence of "non-separated" and "separated" flow regimes was to be tested using a flow visualization technique first presented by Baker in 1966 (22). The technique is described in detail later. It was thought

that if the flow visualization technique proved successful an attempt could then be made to measure the boundary layer widths and also the flow velocities within the boundary layers.

2.2 Experimental Apparatus

Since the primary objective of the experiments was to verify the existence of "separated" and "non-separated" flow fields in the bidirectional flow region, the apparatus was designed to enable test conditions to be reached in as short a time as possible. The design chosen was not suited for the measurement of local heat flux. Considerable effort was placed on perfecting the flow visualization apparatus. A detailed description of the apparatus used in the experiment follows.

2.2.1 The Plate

The plate consisted of four sections; two guard sections and two test sections. The test sections were four inches wide. One section was four inches high and the other six inches. The guard sections were one inch wide by ten inches high. All were cut from a copper plate one-quarter inch thick. The pieces were first cut roughly and then milled to the dimensions given in Figure 4. The plate provided test sections of four inches, six inches, and ten inches high by four inches wide. The guard sections were designed to reduce the edge losses from the test sections, enabling a uniform temperature to be maintained across the plate test surface.

The surfaces of the copper sections were machined

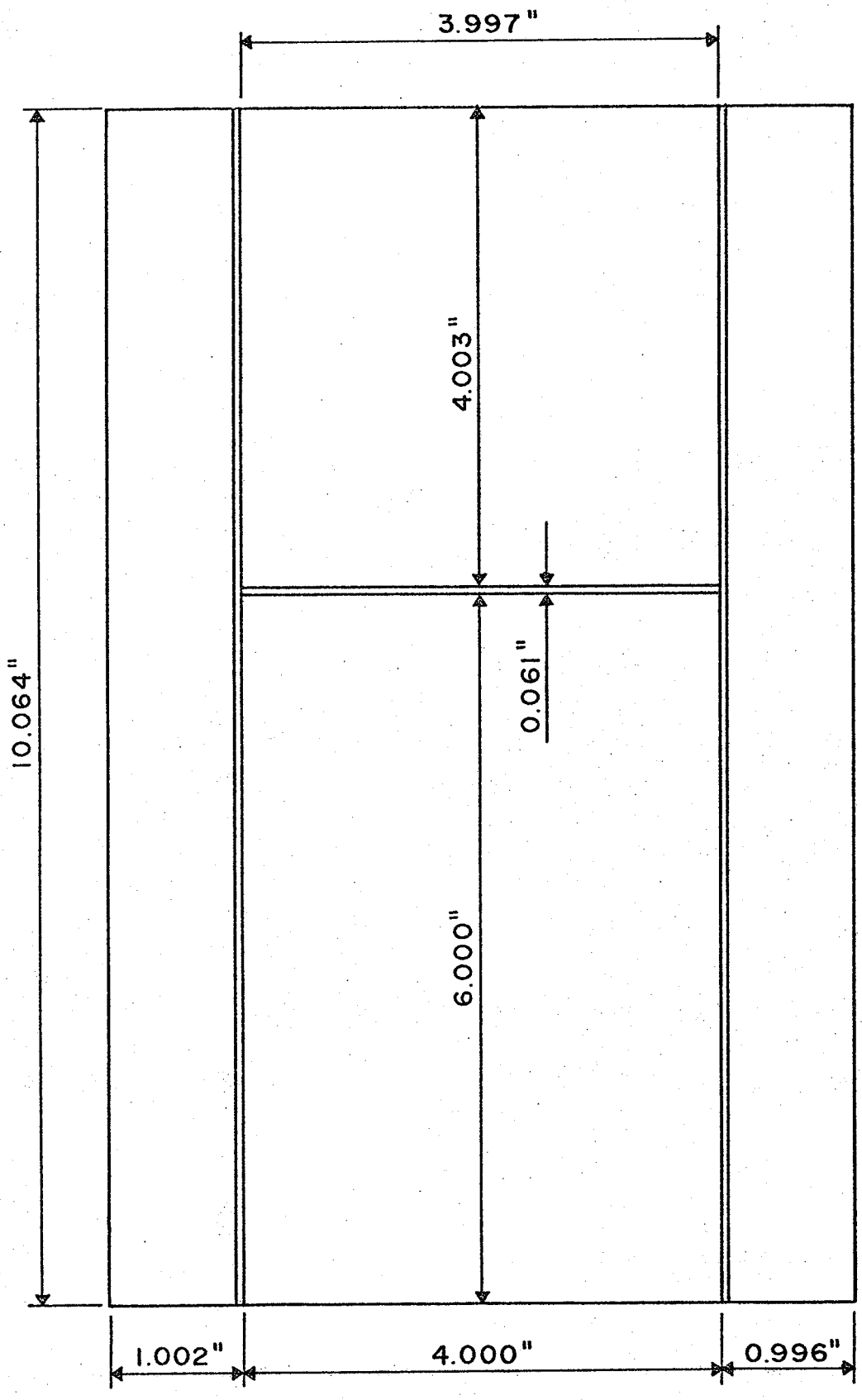

FIGURE 4 PLATE DIMENSIONS

using a special surfacing head in a vertical milling machine. The surfaces were then polished using fine emery cloth. Dowel pin locating holes were drilled in the copper sections to provide a means of joining the sections in a perfectly flat test surface.

Prior to assembly of the plate, thermocouple holes were drilled in the plate as indicated in Figure 5. The holes were drilled as close to the surface as possible. A slitting saw was used to cut thermocouple wire guide grooves. The wires could then be run to one side of the plate and the heaters mounted flush with the plate surface.

The sections of the plate were assembled using a waterproof epoxy cement. After assembly the plate was visually checked for flatness using a straight edge. (No visible deviations could be detected.) The test surface was polished to a mirror finish.

Thermocouples for the plate were fabricated using 30 AWG copper-constantan thermocouple wire. Thirty of these thermocouples were cemented into place on the plate using Minco Type No. 6 RTV silicone base heater cement and numbered in sequence as shown in Figure 5. The thermocouple wires were cemented into the grooves in the plate and the leads run to one side of the plate.

Minco brand electrical resistance heaters were used. The heaters are thin etched thermofoil sections which have

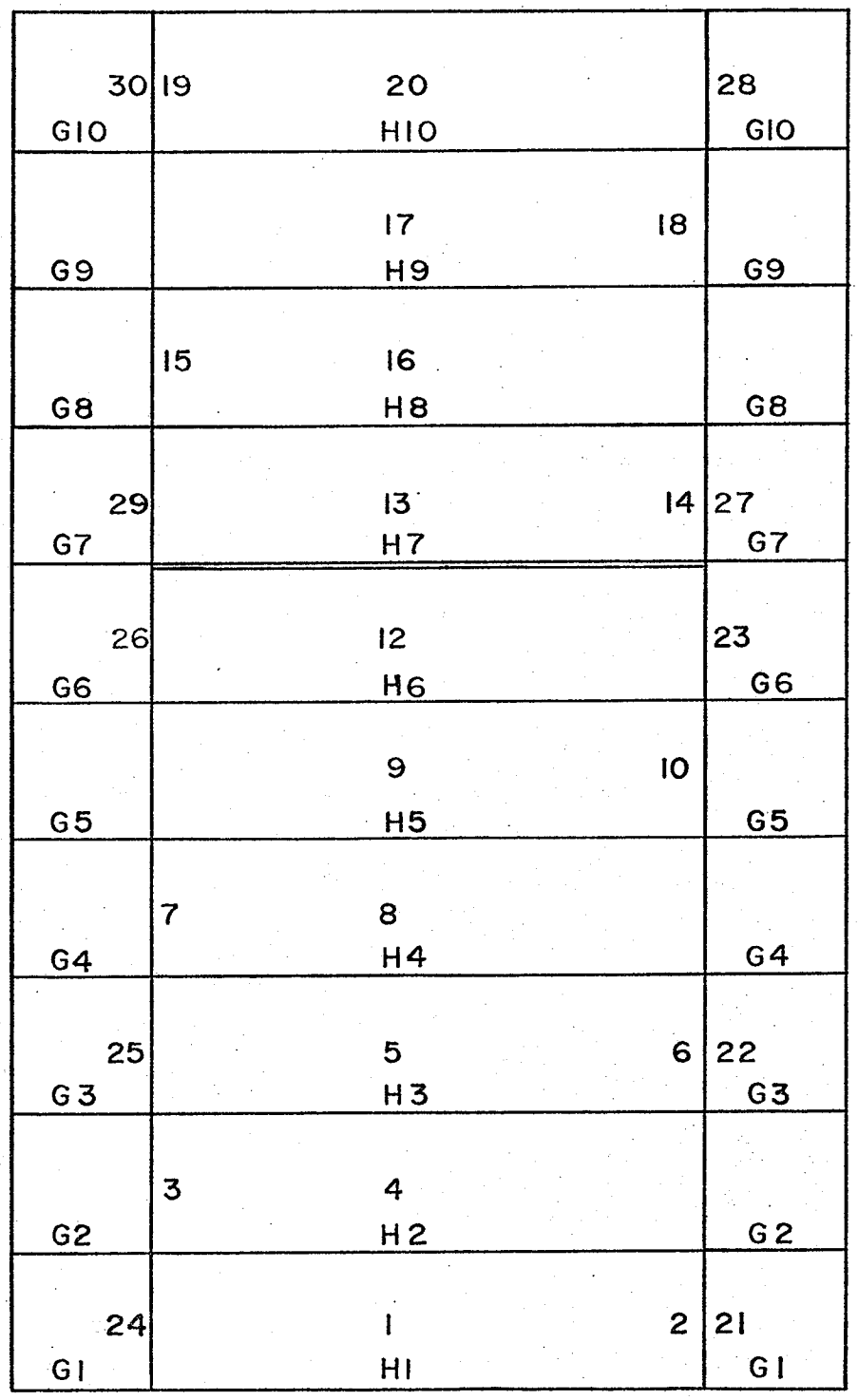

FIGURE 5 THERMOCOUPLE AND HEATER LOCATIONS

a constant heat generation rate. The thermofoil sections are coated with silicone rubber. The ten main heaters were each one inch by four inches and had a nominal electrical resistance of 3.70 ohms. They were mounted on the center section of the plate using Minco Type No. 6 RTV silicone base heater cement. The guard heaters were each one inch by one inch with a nominal resistance of 1.76 ohms. Ten were mounted on each guard section of the plate. The guard heaters at each one inch height of plate were wired together in series.

A calibration check of heater resistances showed that at maximum and minimum powers the resistances varied considerably. Individual heater resistances were calculated as a function of temperature and these "corrected" resistances used in the analysis of power data. The variation of heater resistances is given in Appendix I.

Polyurethane foam was used to insulate the back of the plate. A large piece of foam was cut into sections measuring 11" x 7" x 1". Before the foam insulation was cemented to the heaters a calculation was made to determine the length of heater leads necessary to generate sufficient heat within the block to balance the heat conducted through the thermocouple leads, heater voltage taps, and power leads. The length of leads necessary was found to be 1.2

feet.

The thermocouple wires were run to one side of the main heater section and the heater leads were run to the other. The first layer of foam was put on in two pieces. Holes were punched in one foam piece and the heater leads guided through. This section of foam covered from one edge of the plate up to the thermocouple wires. A small section of foam covered the remaining guard heater section. The foam was bonded to the heaters using the heater cement. The remaining layers of foam were bonded using Minnesota Mining and Manufacturing (3M) Contact Cement.

The power leads and voltage taps were connected to the heaters using two sets of terminal strips. One set was used for the main heaters and the second for the guard heaters. Both were embedded in the foam. One side of each heater circuit was common. One wire from each heater was joined in a "bus-type" clamp to which a flexible stranded welding cable (6 AWG) was also fastened. Voltage taps across each heater were taken from the terminal strips. The length of lead wire from each heater to the terminal strip was less than 6 inches.

Six layers of 1" thick foam were then applied on top of the first layer. Each layer was cut to accomodate the terminal strips and to allow for the power leads to be

wound around the layers. After the second layer, all the wires were grouped. The final layer of foam was not cut in two pieces. Rather, a hole was cut in the center and the leads fed through. A special PVC fitting was screwed into the hole and cemented in place.

The leads were placed in a rubber tube that was fastened to the PVC fitting with a metal hose clamp. This insured a waterproof seal at the exit from the block.

The excess foam was trimmed such that the foam block dimensions were ½ inch larger than the plate dimensions in height and width. Fiberglass mesh and resin were applied to all surfaces of the foam block in several layers to provide a strong and waterproof case for the copper plate test surface, the heaters, and associated electrical hardware.

2.2.2 The Heater Controls and Circuitry

For ease of control and also because thermocouple temperature sensing was used, direct current was used to power the heaters. A Hewlett Packard Model HP Harrison 6260 high current, low voltage direct current power supply was used.

A schematic of the main heater and guard heater circuits is given in Figure 6. For the main heaters a high current capacity, low resistance (0-5 ohm) rheostat

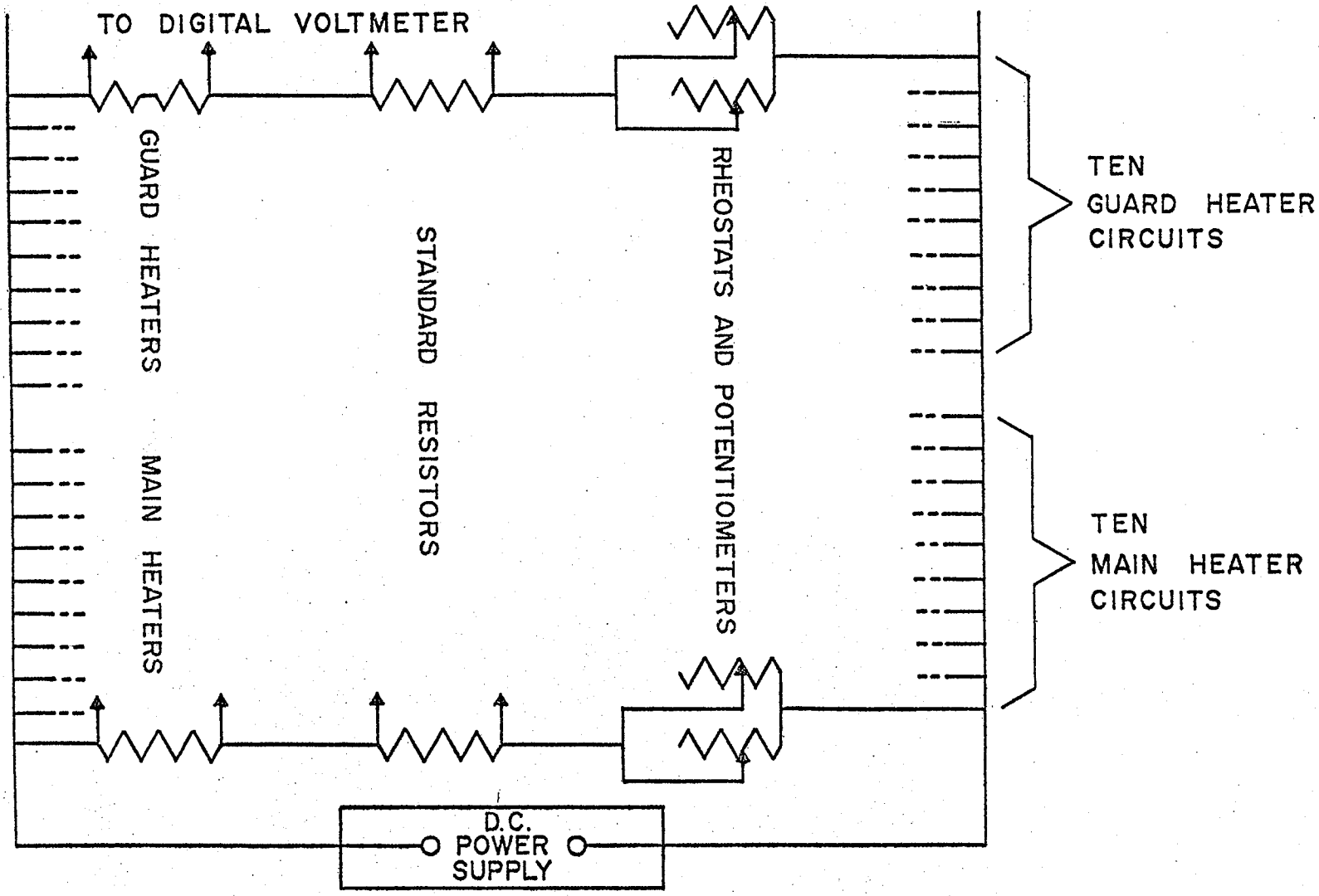

FIGURE 6 SCHEMATIC OF MAIN AND GUARD HEATER CIRCUITS

was used for rough power control. Most of the current flow would be through this rheostat. A ten-turn 0-50 ohm Amphenol potentiometer connected in parallel with the rheostat was used for fine adjustment of the heater power. For the guard heaters an identical circuit was used with a 0-7.5 ohm rheostat in place of the 0-5.0 ohm rheostat.

A 0.5 ohm standard resistor was wired in series with each set of heater and control resistors. The standard resistor was used to provide an accurate measure of the current flowing through each heater circuit. Voltage taps were attached to each standard resistor terminal. The standard resistors were mounted on an aluminum sheet and placed in a bath of mineral oil to maintain them at a constant temperature. The manufacturer's advertised tolerance of the resistance of each resistor was 1%.

Also connected in series with the standard resistors and heater controls were "in-line" fuses. The fuses provided protection against damage to the heaters due to short circuiting of the heater wiring. They also provided a means of controlling the number of heaters in operation for a test.

The heater controls were mounted in the Hammond Turret illustrated in Figure 7. One side of the control circuit was a common and was connected to one side of the D.C.

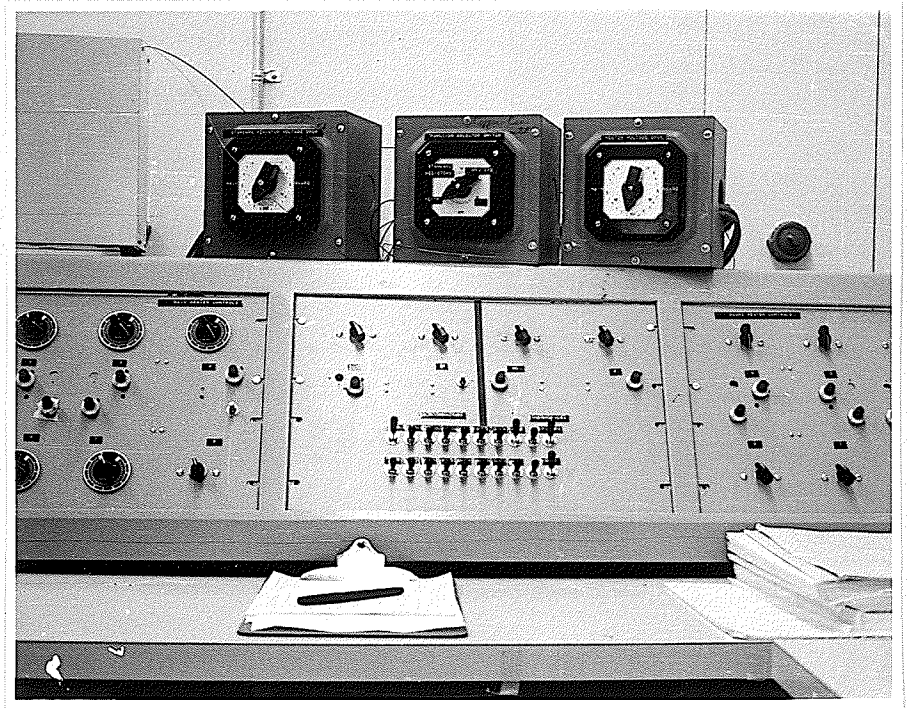

FIGURE 7 CONTROL TURRET

power supply while the common lead from the fiberglass block was connected to the other side of the power supply.

All wires from the individual side of the heater control circuits were soldered to female plug sockets that were in turn mounted at the rear of the turret. The standard resistor voltage taps were also soldered to sockets mounted on the turret.

All the leads from the fiberglass block except the thermocouples were soldered into male plugs. The leads from the block to the cabinet power supply circuits were connected using eighteen foot extension leads.

2.2.3 Temperature and Voltage Drop Measurement

The copper-constantan thermocouples (30 AWG) were mounted as close to the surface of the plate as was physically possible. A Thermo-Electric fixed point cold junction was used with the plate thermocouples. The plate thermocouples were connected directly to compensated terminal strips in the turret.

The bulk water temperature was measured using three thermopiles mounted at different heights in the test tank. The thermopiles were fabricated using Thermo-Electric 20 AWG copper-constantan thermocouple wire. Nine junctions were included in each of the piles. The piles were mounted in "L" shaped glass tubes. The junctions were arranged in

a "starburst" pattern. The end of each glass tube was filled with RTV silicone rubber cement to fix the couples in position in the glass tube. The glass tubes were mounted in an adjustable plexiglass holder that permitted placement of the piles at different heights in the same vertical plane.

The cold junctions for the piles were kept in a distilled water ice bath in a thermos bottle in the cold-room. The leads were connected to compensated terminal strips within the cold room and thermocouple wire was connected to the turret from these strips.

A Hewlett Packard Model HP 3440A Digital Voltmeter and a Leeds and Northrup Model K-5 Potentiometer were used for the voltage measurements. The digital voltmeter was used for the measurement of heater voltages and for rough thermocouple readings.

To permit measurement of the main and guard heater voltage drops, main and guard heater standard resistor voltage drops, plate thermocouple emfs, and the thermopile emfs a complex switching arrangement was designed. One Honeywell Model 911AZ 4 pole switch was used to switch between the different inputs. The three positions used were for the heater voltages, the standard resistor voltages and the thermocouple/thermopile emfs. The wiring in the

box was fully compensated for use with copper-constantan thermocouples. Copper wire of thermocouple grade was used to connect the switch device to the measuring instrument.

Two similar Honeywell switch boxes were wired to accomodate twenty inputs. One box was used for heater voltage drops and the other for standard resistor voltage drops. The leads from each box were wired into male connectors so that they could be plugged into the female connectors mounted at the back of the control turret.

Thermo-Electric double-pole double-throw compensated thermocouple selector switches were mounted on the center panel of the control turret. The switches were wired using thermocouple wire and thermal free solder. Fifteen switches were wired for the plate thermocouples and two for the thermopiles. The switch leads were connected into Thermo-Electric compensated terminal strips. Provision was made in the wiring for the inclusion of a single cold junction for the plate thermocouples. The use of the terminal strips allowed for easy connecting and disconnecting of the switching devices and the thermocouples. The thermocouple selector switches were enclosed in a box of insulating foam to eliminate the possibility of thermal emfs, caused by temperature gradients in the turret, affecting the readings.

2.2.4 The Tank

The ideal medium for testing purposes is an infinite body of water. In laboratory testing, one must provide a practical compromise between that which is feasible and that which is ideal. The tank was designed to minimize the effects of a finite body of water.

A stainless steel tank measuring 3 feet high by 3 feet by 1 foot was fabricated from a sheet of 22 AWG stainless steel. "Window" holes, 2 feet by 2 feet, were cut out of each side six inches from the bottom and centered with respect to the ends of the tank. A hole 8 inches by 2 feet was cut in one end of the tank 6 inches from the bottom. A drain piece was fitted into the tank bottom at the opposite end.

A 1 inch thick plywood box was built to fit snug around the stainless steel tank. Window holes were cut in line with those in tank. Supports of 2 inch by 4 inch lumber were mounted around the window holes. A support stand was also fabricated out of 1 inch plywood. The support stand served to damp out the high frequency motor and compressor vibrations on the floor of the test room.

Optically flat ¼" plate glass windows were mounted in the tank using silicone rubber cement. The window

dimensions allowed for a one inch wide sealing surface on the stainless steel.

2.2.5 The Cold Room

A Coldstream cold room was used for the tests. The temperature range of the room was from - 18°C to 24°C. The limits of control were ±½°C. Inside dimensions of the room were 9 feet by 12 feet. Access ports were installed on the three exposed sides of the room.

2.2.6 The Flow Visualization Technique

The thymol blue flow visualization technique was first used by Baker (22) in 1966. Sparrow and Husar (23) in 1969, and Lloyd and Sparrow (24) in 1970 used the technique to study natural convection flow on inclined heater plates.

In the technique a pH indicator, thymol blue (thymol-sulphonepthalein), is added to distilled water to produce a 0.01% (by weight) solution. The solution is titrated to the end point by addition of 1N-NaOH drop by drop until the solution turns deep blue, then adding one drop of 1N-HCl to cause the solution to be on the acid side of the end point.

In several preliminary tests it was found that a 0.01% (by weight) solution was too dark for the width of the test tank used. The concentration of the thymol blue was reduced to 0.006% by weight to give a solution that

would provide sufficient contrast for photography under limited lighting conditions.

The dye is produced in the solution by impressing a potential of 15-20 volts across two electrodes for a time period of approximately five seconds. A proton transfer is induced at the cathode. There is a change of pH from acid to base at the surface of the negative electrode and hence a change in colour from yellow-orange to blue. The dye is neutrally bouyant and will faithfully follow the motion of the fluid.

2.2.7 Plate Support and Dye Producing Probe

The plate was supported on a 14 AWG galvanized metal support as illustrated in Figure 8(a). The base of the support was large enough that a weight could be placed on it to hold the support and plate on the tank bottom. The block was very bouyant due to the low density of the polyurethane foam insulation.

A plexiglass frame was built around the fiberglass block and fastened to the metal support stand. The plate could be positioned with either the six inch or the four inch section at the bottom. The sides of the frame were grooved to permit positioning of the dye-producing probe support at various heights along the plate surface.

Several different techniques of fabricating a dye-

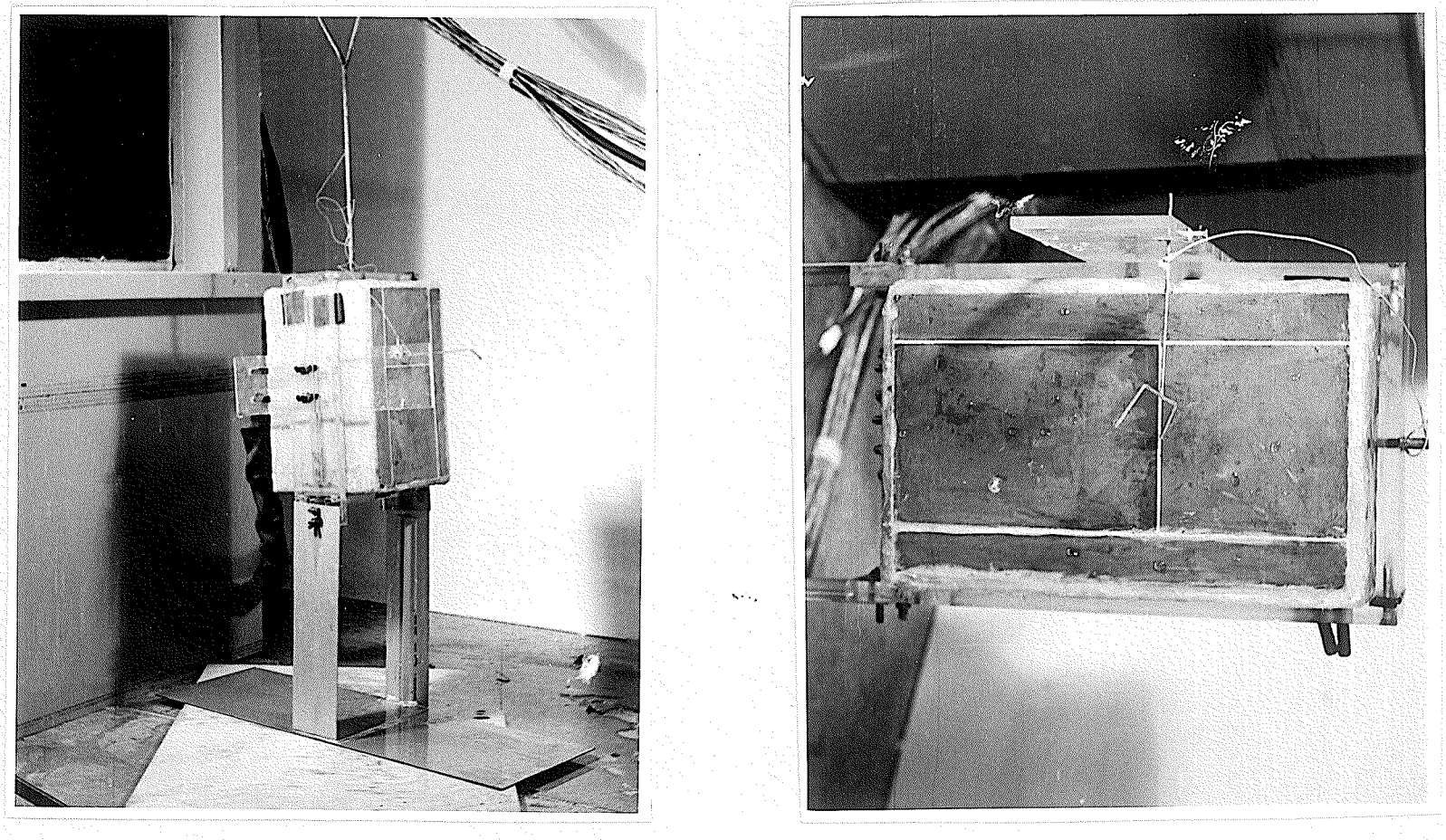

(a) (b)

FIGURE 8 PLATE SUPPORT AND DYE PRODUCING PROBE

producing probe were tried. The probe had to be designed to permit the production of dye in the area immediately adjacent to the plate without disturbing the flow in the vicinity of the plate or coming into electrical contact with the plate. A piece of welding rod was bent in the shape of a distorted "Y" as shown in Figure 8 (b). A 0.0015 inch diameter platinum wire was stretched between the two probe ends and soldered in place. The distorted end of the "Y" was filed to a sharp point and a lead wire attached to the base of the "Y". The welding rod was then coated with a waterproof lacquer to insulate the rod from the thymol blue solution.

Two types of probes were used. The first type was a bare platinum wire and it produced a sheet of dye. In the second type alternate sections of the wire were insulated to produce a "streaked" dye flow. It was thought that a streaked dye flow would be more easily photographed and analysed.

The actual procedures used to produce the dye are documented in the procedure section of this report.

2.2.8 Miscellaneous Equipment and Apparatus

For photography a NIKON 'FTN' 35 mm single lens reflex camera complete with a NIKON Model F 28 battery-powered

motor drive was used. Several different lenses were available and were tried - 28mm, 50mm, and 135mm. Kodak Tri-X film (400 ASA) was used for all the tests.

For lighting, both a single fluorescent tube and a bank of fluorescent tubes were used. Fluorescent lighting provided a diffuse light with no addition of heat to the tank. A concentrated light source such as a spotlight would have provided more contrast but would have introduced stray thermal convective currents into the tank.

2.3 Experimental Procedure

2.3.1 Procedure for Heat Transfer Measurements

In the experiments a nine cubic foot tank of water was used to simulate an infinite medium. The major obstacle to be overcome in conducting the heat transfer tests was to carry out all the adjustments and data logging before the buildup of heat in the tank would begin to affect the boundary layer flow on the plate. It was necessary: to adjust 20 heater circuits to obtain an isothermal plate, to measure the voltage drops across 20 standard resistors, to measure the emf of 30 plate thermocouples and three thermopiles, and to allow time for the steady state to be reached in the plate, insulation, and boundary layer.

The plate power, including both main heaters and guard heaters ranged from 20 watts to 60 watts. With a tank volume of 255 kg of water the maximum expected rate of temperature rise in the tank, assuming no heat removal, would be $0.20^{o}C/hr$.

In free convection studies in water below $4^{o}C$ a layer of heated water, well above $4^{o}C$, builds up at the top of the tank. However, this layer of heated water is not stable. As it cools to near $4^{o}C$ it becomes denser and sinks through the bulk fluid to the bottom where a layer of heated water near $4^{o}C$ builds up.

Hence in conducting the tests which followed the investigators had to keep in mind at all times the peculiar behavior of the water. The plate assembly was centered in the tank. Sufficient space both above and below the plate was provided to allow for the build up of the heated layers.

Yuill's experimental correlations in Regions II-S and II-N (1) were used to generate tables of local heat transfer coefficients as a function of plate and bulk temperatures. These coefficients together with heater areas, heater resistances, and standard resistor resistances were used to calculate the required standard resistor voltage drop for a given heater power. Both main and guard heater voltage drops were calculated. To account for edge losses from the guard heaters, the guard heater voltage drops were increased by an experimentally determined 7% multiplication factor.

The cold room was set at the desired temperature and the tank brought to thermal equilibrium with the room. The water was stirred continuously by an electric mixer during the above process. When the room and tank reached thermal equilibrium the mixer was shut off. When the water in the tank was motionless, as indicated by a few neutrally bouyant spheres in suspension, the test was ready to begin.

The calculated voltage drops were applied to the main and guard heaters using the high current, low resistance rheostats. The wire wound potentiometers were all set at their maximum resistance values to prevent their burnout by overpowering. The power supply voltage was initially set to give the voltage drop for the lowest powered heater. The rheostats had all been initally set at their maximum resistance values. The rest of the heater powers were set by adjusting the rheostats. The power level of the power supply was boosted for a few minutes to decrease the time required to reach steady state. About ten minutes after the power level had been returned to its initial setting and the plate thermocouples at selected points had ceased to change with time, the plate thermocouple readings were recorded and examined. The adjustments required to achieve isothermal conditions on the plate were calculated from the thermocouple deviations of the plate. Adjustments were made to the heater powers using the wire wound potentiometers. The procedure was repeated until isothermal conditions were achieved.

The plate thermocouple emfs were then recorded along with thermopile emfs, main and guard heater standard resistor voltage drops. The thermopile emfs were examined several times while the attempts were made to achieve an

isothermal plate.

The above procedure did not prove to be satisfactory as considerable time was required to attain an isothermal condition on the plate. Yuill's predicted heat transfer coefficients (1) were in considerable error at the top and bottom of the heated section. It was felt that there was insufficient time available to continually adjust the upper and lower heaters.

The addition of ice to the top of the tank was not permissible as this would have altered the concentration of the thymol blue dye. Ice would have absorbed some of the energy of the rising plume of hot water, and decreased the rate of temperature rise in the tank.

Yuill (1) gave actual experimental heat transfer coefficients for several of his tests in Region II-S. It was decided to use Yuill's experimental heat transfer coefficients to calculate the required power inputs to the heaters used in the present investigation.

A test was selected and the required guard and main heater standard resistor voltage drops calculated. The bulk temperature was adjusted to the required temperature as previously mentioned. The previously described procedure of adjusting the heater powers and running the test was then followed.

Several additional tests were run by adjusting the bulk temperature or plate temperature slightly about Yuill's test points. Minor adjustments were required in the heater powers. The above procedure was adopted for the balance of the test program. The test numbering sequence was chosen to reflect the collection of tests about Yuill's test points. The distribution of test results will be discussed in a later section of this report.

The test program was conducted in two parts. In the first part, conducted by the author, the test procedure was established and about one-half of the tests conducted. The second part of the research program was carried out by two research assistants who were instructed to follow the established procedure and collect results throughout Regions II-S and II-N.

During the tests several problems developed in the apparatus. The seal between the copper plate and the fiberglass epoxy began to leak and water began to penetrate into the space between the polyurethane foam and the fiberglass covering. Several times the plate assembly had to be removed from the tank, drained, dried out, and sealed using paraffin wax.

The epoxy cement that had been used to seal the copper sections of the plate began to crack and leak in a few

places. Wax was melted into the leaks and the excess scraped off to ensure a smooth test surface.

The tank began to leak along the seal between the windows and the stainless steel. These leaks were sealed using silicone rubber cement.

In summation, the above problems with the apparatus necessitated the cutting short of the test program. However, sufficient data had been collected to achieve the objectives stated earlier.

2.3.2 Flow Visualization Technique

The thymol blue flow visualization technique was described in general terms in section 2.2.6 of this report. The following is a description of the procedure used in the experimental program to obtain dye traces of the free convection flow patterns.

A 0.006% by weight solution of thymol blue and distilled water was prepared and titrated to the end point using 1N-NaOH and 1N-HCl. A plate 6 inches by 6 inches was used as the anode. Two different cathodes - one plain and one beaded - were used in the tests. They are described in Section 2.2.7 of this report.

The amount of dye produced at the probe wire is related to the potential impressed upon the circuit and the time for which it is applied. Baker (22) had

recommended the use of a potential of 5 V DC for an electrode spacing of 0.5 cm. Sparrow and Husar (23) reported the use of a potential of 10-20 volts DC. For initial tests in the present investigation a potential of 26 V DC was applied for 3 - 5 seconds. In later tests the applied potential was reduced to 20 V DC and the duration to one second.

In some tests problems were encountered with the formation of bubbles on the wire. The bubbles would stream off the wire carrying the dye upward with them. It is likely that the bubbles were hydrogen, formed on the wire due to electrolysis of the water. The bubble formation was inconsistent. In the first tests performed by the author at the higher potentials no problems were encountered and the dye traces produced showed no tendency to stream off the wire. Contrast in these tests was excellent and the dye could easily be seen. However, in later tests performed by the assistants problems were encountered with the dye streaming off the wire.

The procedure established was to first set the wire position and make sure that it was perpendicular to the plate. The probe was positioned either at the top of the 6 heater section in the middle of the plate or at the midpoint of the 6 heater section. Before running a test

the wire and plate surface were dusted free of bubbles using a camel hair brush. After the plate temperature had stabilized and the readings had been taken the potential was applied to the probe circuit and photographs taken at either 3 or 5 second intervals.

The thymol blue solution had to be titrated to the end point several times. As the test program proceeded the thymol blue solution became progressively darker and even titrating would not improve the colour.

In the last few tests of the present experimental program it was not possible to obtain photographs. However, in these tests the flow patterns were observed by Yuill and the research assistants. Their descriptions of the flow patterns they observed are included in the discussion of results.

The distribution of flow visualization results is discussed in section 3.2.1 of this report.

CHAPTER 3

ANALYSIS OF RESULTS

3.1 Heat Transfer Results

3.1.1 Distribution of Results

In this experiment data was collected at 48 different points throughout Region I and II. In the 5 tests performed in Region I the height of the heated plate was 25.563 cm (10.064 in.) as measured with vernier calipers.

In Region II-S 4 tests were performed with a plate height of 25.563 cm and 38 tests with a heated plate height of 15.24 cm (6.00 in.). A 15.24 cm heated plate height was used for the one test performed in Region II-N. The plate and bulk temperatures at which measurements were made are given in Figure 9.

3.1.2 Data Processing

The raw experimental data from the tests was first processed using a computer program that converted the thermocouple and thermopile emfs and standard resistor voltage drops into temperatures and heater powers. The mean and root mean square (rms) deviations from an isothermal plate were calculated for each test and the results are presented in Table I. The mean of the absolute values of the deviations of the local plate temperatures from the mean plate temperature varied from a high of 6.72% in

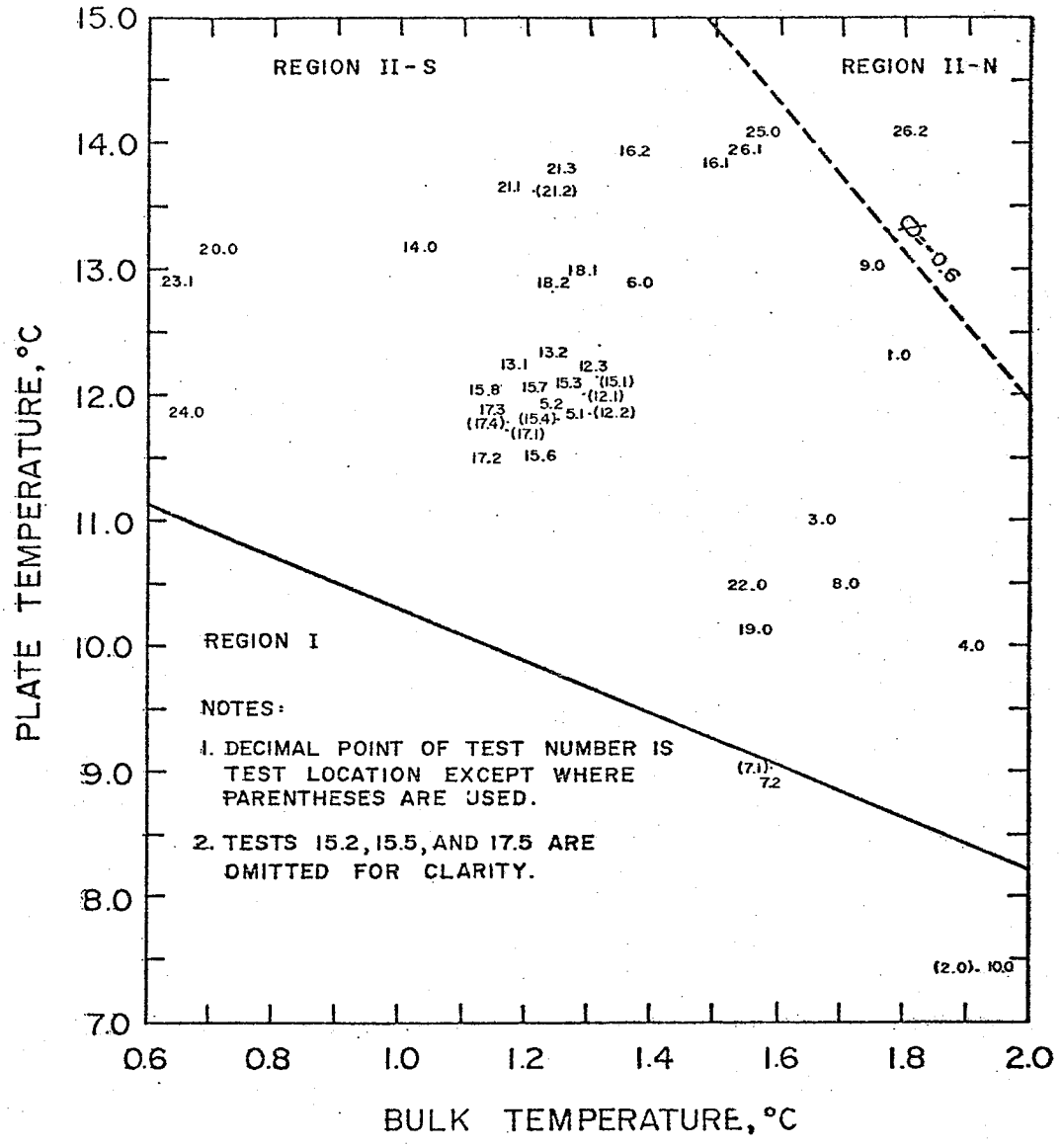

FIGURE 9 LOCATION OF EXPERIMENTS

TABLE I

DEVIATIONS FROM AN ISOTHERMAL PLATE

TEST NO.	HEATERS	Θ_p	MEAN DEVIATION, %	RMS DEVIATION, %
1.0	10	10.51	5.54	5.85
2.0	10	5.50	1.10	1.63
3.0	10	9.30	5.74	6.01
4.0	6	8.06	1.19	1.73
5.1	6	10.56	.75	1.19
5.2	6	10.66	.91	1.21
6.0	6	11.49	1.33	2.12
7.1	10	7.43	1.32	1.58
7.2	10	7.19	1.01	1.18
8.0	10	8.76	6.72	7.01
9.0	10	11.25	.97	1.70
10.0	10	5.44	2.15	2.65
11.0	10	8.46	1.54	1.93
12.1	6	10.72	2.64	2.91
12.2	6	10.55	1.28	1.69
12.3	6	10.89	1.21	1.65
13.1	6	11.03	.84	.95
13.2	6	11.06	.87	1.02
14.0	6	12.11	.80	.90
15.1	6	11.00	1.00	1.13
15.2	6	10.7	.62	.83
15.3	6	10.8	.65	.89
15.4	6	10.56	.67	1.12
15.5	6	10.77	.69	1.20
15.6	6	10.25	.79	1.32
15.7	6	10.81	.71	.94
15.8	6	10.86	.74	1.04
16.1	6	12.31	1.44	2.23
16.2	6	12.55	1.27	1.92
17.1	6	10.57	.71	.97
17.2	6	10.32	.70	1.02
17.3	6	10.70	.77	.91
17.4	6	10.62	.85	1.11
17.5	6	10.58	.90	1.22
17.6	6	10.59	.78	1.03
18.1	6	11.67	.78	1.19
18.2	6	11.61	.69	.89

TABLE I CONT'D.

DEVIATIONS FROM AN ISOTHERMAL PLATE

TEST NO.	HEATERS	θ_p	MEAN DEVIATION, %	RMS DEVIATION, %
19.0	6	8.54	1.57	1.99
20.0	6	12.41	1.14	1.61
21.1	6	12.45	.93	1.17
21.2	6	12.42	.91	1.07
21.3	6	12.50	1.04	1.28
22.0	6	8.89	1.05	1.20
23.1	6	12.22	.83	.97
24.0	6	11.17	1.14	1.31
25.0	6	12.47	.99	1.41
26.1	6	12.38	1.07	1.34
26.2	6	12.25	.97	1.26

Test 8.0 to a low of 0.62% in Test 15.2. The rms deviations of the local plate temperatures from the mean ranged from 7.01% to 0.83%.

The power applied to the heaters in the test section was calculated from the standard resistor voltage drops and heater resistances. Assuming that heat losses through the insulated block were negligible and that all the power applied to the heaters in the test section was transferred through the copper test section to the water it was a relatively simple matter to calculate the mean heat transfer coefficient for each of the tests. It was not possible to measure local heat fluxes with the apparatus and thus in a comparison with Yuill's results (1) only mean values can be compared.

3.1.3 Examination of Results in Region I and Comparison with Yuill's Analytical Model for Region I

The results of the tests performed in Region I are presented in Table II. The mean experimental heat transfer coefficient ranged from 111.825 watts/m^2 ^oC to 140.213 watts/m^2 ^oC.

The mean theoretical heat transfer coefficients were calculated by using Yuill's analytical model (see page 17 Eqn. 1 - 10) to evaluate the coefficient C_I. The equation for the local Nusselt number, Nu_x, Eqn. (1-8) was

integrated over the plate surface to find $\overline{Nu}$ and thus $\bar{h}$. The theoretical mean heat transfer coefficients are given in Table II.

The mean of the percentage deviations of the experimental values of the mean heat transfer coefficient from the predicted values is 4.71%. The root mean square deviation (rms) is 6.06%.

The two tests in which the percentage deviations are the highest are close to the Region I - Region II boundary. It is not clear why the deviation is greater at this point since the correlation for C versus $\propto$ matches the analytical data at the Region I - Region II boundary.

Yuill (1) only had two tests in Region I. He chose to compare the mean value of the experimentally determined coefficient C_I along the plate for a particular test with the theoretical. In his test the rms of the percentage deviations of the experimental C values from the predicted values was 7.95%.

The analytical work in Region I done by Yuill (1) used a well tested technique and compared favourably with previous work done in the same region. Therefore, it was thought that comparison of the present experimental results with Yuill's analytical model and experimental results could be considered as a check on the accuracy of the

TABLE II

COMPARISON OF EXPERIMENTAL AND ANALYTICAL HEAT TRANSFER RESULTS IN REGION I

Test No.	Plate Temp.	Bulk Temp.	$\overline{h_T}$, $\frac{\text{watts}}{m^2\ ^oC}$	$\overline{h_e}$, $\frac{\text{watts}}{m^2\ ^oC}$	$\frac{\overline{h_e}-\overline{h_T}}{\overline{h_T}}$, %
2.0	7.42	1.92	114.3	118.9	+ 4.0
7.1	9.02	1.59	113.6	123.4	+ 8.7
7.2	8.78	1.59	116.8	127.5	+ 9.2
10.0	7.40	1.96	112.8	111.8	- 0.9
11.0	9.42	0.96	136.8	140.2	+ 2.5

NOTE: All Region I tests were performed using a plate height of 25.563 cm (10.064 in.)

present experimental apparatus and experimental work.

3.1.4 Examination of Results in the Region of Bi-directional Flow, and Comparison with Yuill's Correlations

The experimental results in Region II were examined to see if the test results could be grouped into regions of "separated" and "non-separated" bidirectional flow. For the tests in which six heaters had been employed, the rate of decrease of temperature along the adiabatic section of the plate above the heated section was examined. The percentage change of temperature from the last heated section to the first unheated section varied from 67.483% to 82.099% for 37 tests and was 33.336% for one test. The decay of temperature along the adiabatic section is given in Appendix II.

The test locations are given on a plot of plate temperature versus bulk temperature (Figure 9). The scales on the plot have been expanded to facilitate examination of the results. Yuill (1) had designated the line $\phi = -0.6$ as the dividing line between "separated" and "non-separated" flow. Examination of test locations reveals that the data from the present experiment fits Yuill's hypothesis.

Results from the ten-heater tests are also plotted in Figure 9. It has been assumed that these exhibit

separated flow since they are located in Region II-S of the plot.

The one test that falls in Region II-N, Test 26.2, exhibits a percentage change of temperature of only 33.3%. This would tend to indicate that the inner boundary layer has indeed extended past the top of the heated section to insulate the unheated section from the bulk water.

The mean experimental heat transfer coefficients were calculated and are present in Table III. Mean experimental heat transfer coefficients range from a low of 107.8 watts/m^2 ^oC to a high of 164.1 watts/m^2 ^oC.

The test results in Region II-S were compared with predictions made by using Yuill's correlation, Equations (1-14) to (1-18), of this report.

Yuill's correlation can be used to generate local values of the heat transfer coefficient. In order to obtain the mean heat transfer coefficient the local values had to be numerically integrated over the heated plate length. A basic language computer program was written and run on the University of Manitoba Department of Mechanical Engineering's Hewlett Packard Model 2116C minicomputer. The program generated the local values and mean value of the heat transfer coefficient.

The predicted heat transfer coefficients, designated

h_T, are presented in Table III, along with the experimental coefficients and percentage difference between experimental and predicted coefficients. For the tests with a heated plate length of 25.563 cm (ten heaters) the percentage deviations of the mean experimental heat transfer coefficients from the predicted range from -9.28% to -2.68% with the mean of the per cent deviations being -6.00%. The rms deviation is 6.44%.

For the tests with a heated plate height of 15.24 cm the percentage deviation of the mean experimental heat transfer coefficients from the predicted range from -7.18% to 18.31%. The mean of the per cent deviations is 5.25% and the rms deviation is 7.24% .

When Yuill (1) compared his experimental results in Region II-S with the predictions from his correlations he found that for plate heights of 23.645 cm (10 heaters) his correlation under-predicted the mean plate heat flux by an average of 2.3%. For plate heights of 14.164 cm (6 heaters) he found that his correlation over-predicted the mean plate heat flux by an average of 5.0%. He found that the rms deviation of the mean plate heat flux from the predicted was 6.06%.

In the present study it was found that Yuill's correlation tended to under-predict the heat transfer

TABLE III

COMPARISON OF EXPERIMENTAL RESULTS AND YUILL'S CORRELATION IN REGION II-S

(a) Plate Height = 25.563 cm (10.064 in.)

Test No.	Plate Temp.	Bulk Temp.	$\overline{h_T}$, watts/m^2 ^oC	$\overline{h_e}$, watts/m^2 ^oC	$\frac{\overline{h_e}-\overline{h_T}}{\overline{h_T}}$, %
1.0	12.30	1.79	133.2	124.7	- 6.4
3.0	10.97	1.67	115.2	108.6	- 5.7
8.0	10.47	1.71	110.7	107.8	- 2.7
9.0	13.00	1.75	144.2	130.8	- 9.3

(b) Plate Height = 15.24 cm (6.000 in.)

Test No.	Plate Temp.	Bulk Temp.	$\overline{h_T}$, watts/m^2 ^oC	$\overline{h_e}$, watts/m^2 ^oC	$\frac{\overline{h_e}-\overline{h_T}}{\overline{h_T}}$, %
4.0	9.97	1.91	116.8	124.2	+ 6.3
5.1	11.84	1.28	136.6	145.6	+ 6.6
5.2	11.90	1.24	137.5	144.3	+ 4.9
6.0	12.87	1.38	147.6	154.3	+ 4.6
12.1	12.01	1.29	138.0	151.4	+ 9.7
12.2	11.85	1.30	136.6	153.8	+12.6
12.3	12.20	1.31	139.7	149.1	+ 6.7
13.1	12.22	1.19	140.6	148.8	+ 5.9
13.2	12.31	1.25	141.0	148.4	+ 5.3
14.0	13.15	1.04	150.1	152.6	+ 1.6
15.1	12.31	1.31	140.8	146.5	+ 4.1
15.2	11.95	1.25	137.8	147.7	+ 7.2
15.3	12.07	1.27	138.7	146.4	+ 5.5
15.4	11.81	1.25	136.7	149.6	+ 9.4
15.5	12.02	1.25	138.4	146.7	+ 6.0
15.6	11.48	1.23	134.6	154.0	+14.4
15.7	12.03	1.22	138.7	146.2	+ 5.4
15.8	12.00	1.14	139.4	146.1	+ 4.8

TABLE III CONT'D.

COMPARISON OF EXPERIMENTAL RESULTS AND YUILL'S CORRELATION IN REGION II-S

Test No.	Plate Temp.	Bulk Temp.	$\overline{h_T}$, $\frac{watts}{m^2\ ^oC}$	$\overline{h_e}$, $\frac{watts}{m^2\ ^oC}$	$\frac{\overline{h_e}-\overline{h_T}}{\overline{h_T}}$, %
16.1	13.82	1.51	166.2	163.6	- 1.5
16.2	13.93	1.38	163.7	160.0	- 2.3
17.1	11.74	1.17	137.1	140.4	+ 2.4
17.2	11.46	1.14	136.0	143.7	+ 5.7
17.3	11.85	1.15	138.2	143.1	+ 3.6
17.4	11.79	1.17	137.5	144.2	+ 4.9
17.5	11.78	1.20	137.0	144.7	+ 5.6
17.6	11.79	1.20	137.1	144.6	+ 5.5
18.1	12.97	1.30	148.2	152.4	+ 2.8
18.2	12.86	1.25	146.7	153.1	+ 4.4
19.0	10.11	1.57	122.1	139.0	+13.8
20.0	13.13	0.72	153.4	164.1	+ 7.7
21.1	13.63	1.18	155.7	160.6	+ 3.2
21.2	13.63	1.21	156.0	159.5	+ 2.3
21.3	13.76	1.26	158.4	156.5	- 1.2
22.0	10.45	1.56	123.7	136.7	+10.5
23.1	12.88	.66	152.7	163.0	+ 6.7
24.0	11.84	.67	148.3	175.4	+18.3
25.0	14.06	1.58	175.0	162.4	- 7.2
26.1	13.94	1.56	171.1	160.4	- 6.3

coefficients for plate heights of 15.24 cm (6 heater) and over-predict the coefficients for plate heights of 25.563 cm.

The correlating variables in the equations for the coefficients C_i and C_o which appear in the equation for the local heat transfer coefficient h_x are ϕ and γ. These variables have been defined previously in Equations (1-15) and (1-16).

The variation of per cent error in the prediction of heat transfer coefficients was examined in an attempt to see whether the correlations for C_i and C_o were incorrect or whether the error was due mainly to experimental scatter.

In Figures 10 and 11 the per cent error has been plotted as a function of both ϕ and γ. The per cent error tends to increase as ϕ becomes more negative and as γ becomes smaller. ϕ was defined as the perpendicular distance from the Region II - Region III boundary (positive towards Region IV). γ was defined as the angle of rotation about the point $T_p=4^oC$ and $T_b=4^oC$ with the Region I - Region II boundary assigned a value of $\gamma = 0$. In terms of the plot of plate temperature versus bulk temperature it is evident that the error in Yuill's correlation for Region II-S increases as the Region I boundary is

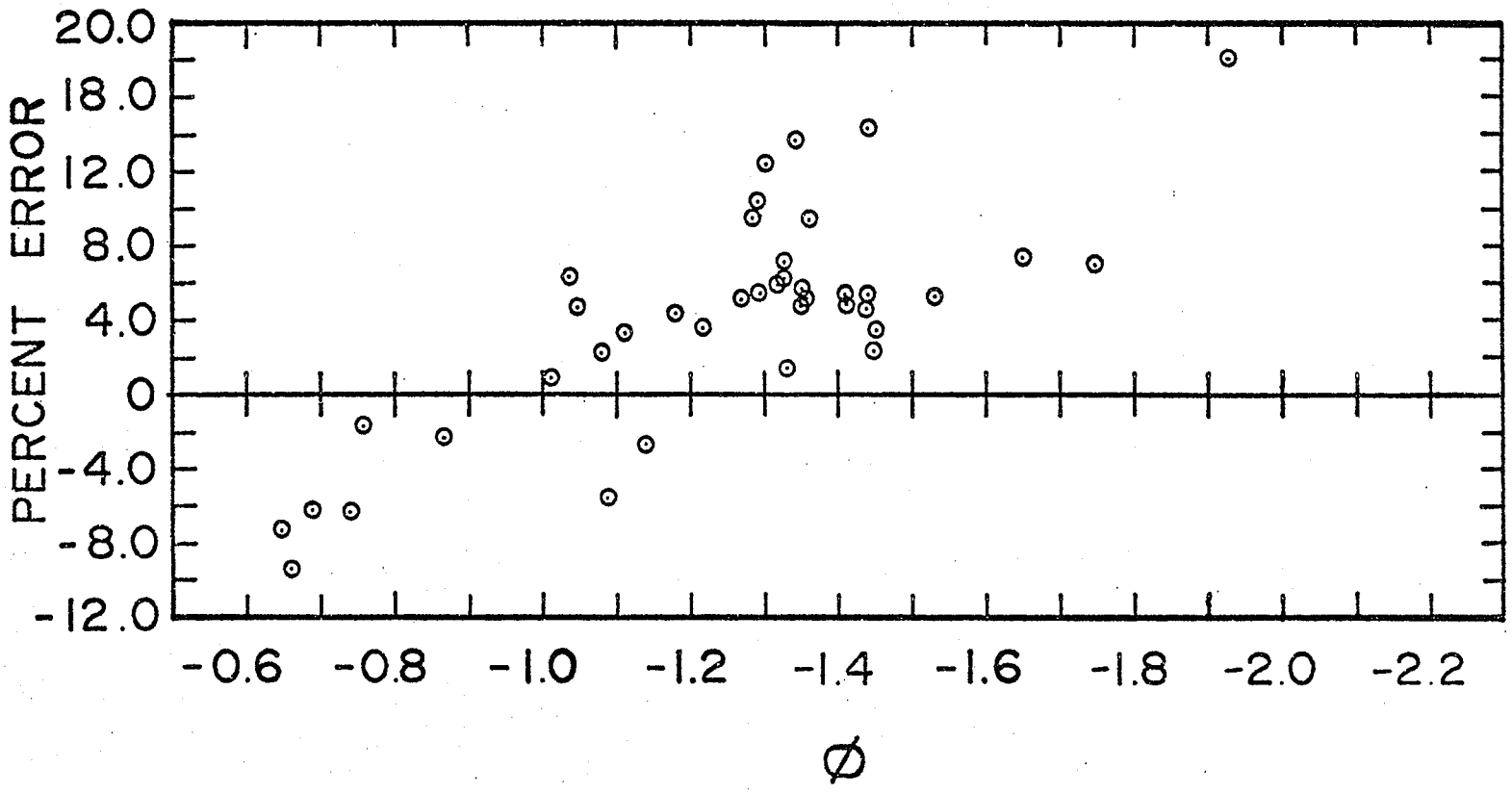

FIGURE 10 PERCENT ERROR vs Ø REGION II - S

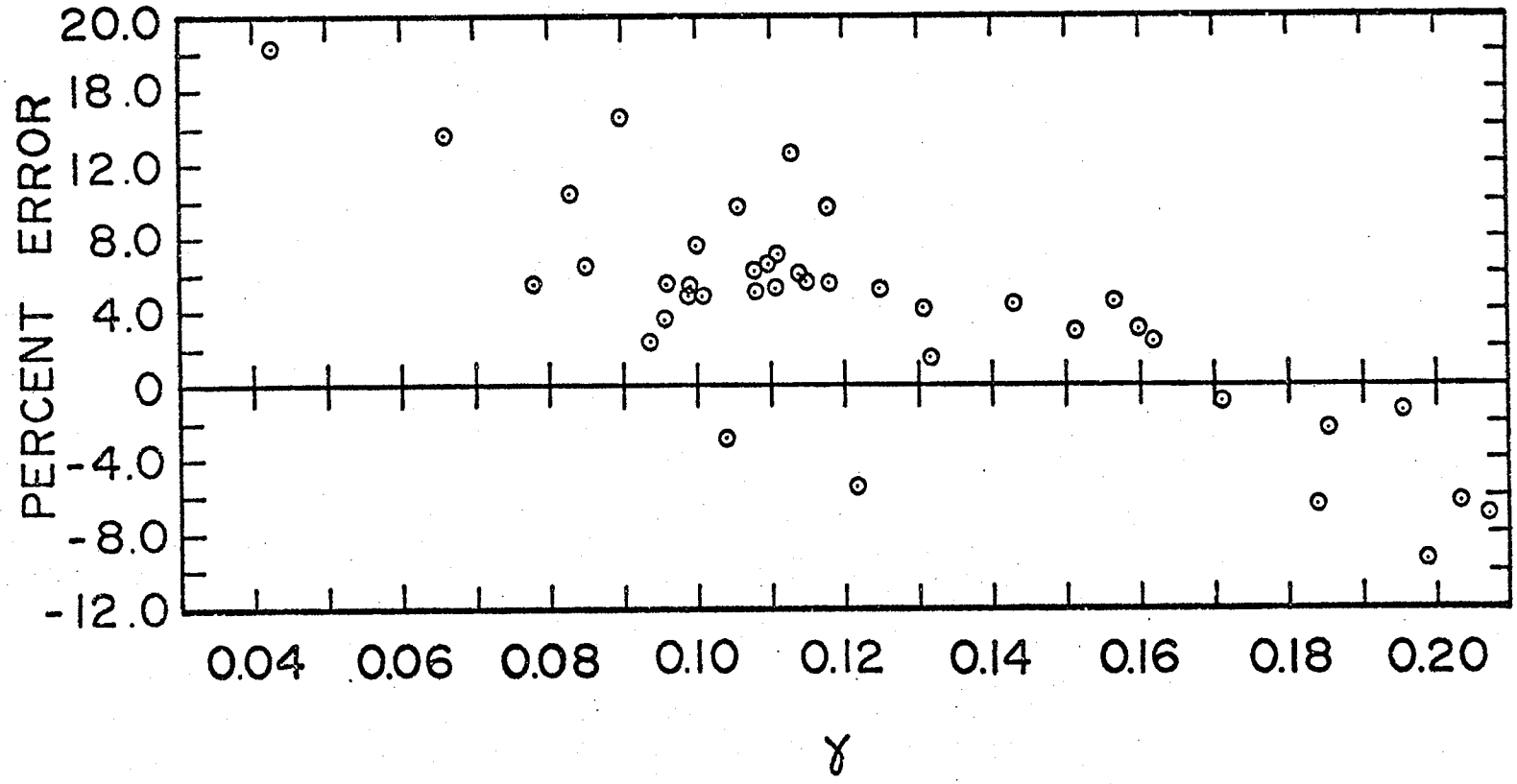

FIGURE II PERCENT ERROR vs γ REGION II - S

approached. The errors suggest that the correlating equations for C_i and C_o require refinement or possibly a change in the form of the equation.

In order to make corrections to the form of the equations more experimental data is required. The data must also include local heat flux measurements. In the present study no attempt was made to refine or correct the correlations.

The effect of plate height was not consistent with Yuill's results (1). In the present analysis the predicted heat transfer coefficients were greater than the experimental results for the ten heater cases by an average of 6.00%. In Yuill's ten heater tests the measured values of heat flux averaged 2.3% above the experimental results. For six heater tests the experimental results averaged 5.25% above the predicted results in the present analysis compared with the 5.0% below in Yuill's tests. This leads one to believe that the correlation requires further refinement to account for the effects of plate height on the heat transfer results.

Due to the technical difficulties previously discussed only one test was run in Region II-N. The experimental heat transfer coefficient for Test 26.2 was 3.38% lower than that predicted by Yuill's correlation given in equations (1-12),(1-13) and (1-14) of this report. In Yuill's

Region II-N tests the rms deviation of the measured values of C_{II-N} from those predicted by the correlation was 6.35%. With only one test for comparison no valid conclusions can be made on validity or accuracy of the correlation.

3.2 Flow Visualization Results

3.2.1 Distribution of Results

All of the flow visualization test results are in Region II and are for a plate height of 15.24cm(6.0 inches). Photographs were obtained in 19 tests. In three additional tests it was not possible to obtain photographs; however visual observations were recorded. The distribution of the test results is given in Figure 12.

The tests can be subdivided into those in which the probe was at the top of the heated section and those in which the probe was at the midpoint of the heated section. In Table IV the probe location, probe type, and photographic interval for the tests are given.

A bare platinum wire probe was used in all tests with the probe at the top of the heated section. Tests in this group include the following: 12.2, 12.3, 13.1, 13.2 and 15.1. The photographs in these tests were taken at intervals of 5 seconds. The quality and contrast of these pictures is excellent.

In Tests 25.0, 26.1, and 26.2 it was not possible to obtain photographs. A bare wire probe, located at the top of the heated section, was used in these tests.

A beaded probe located at the midpoint of the heated section was used in all of the remaining tests except

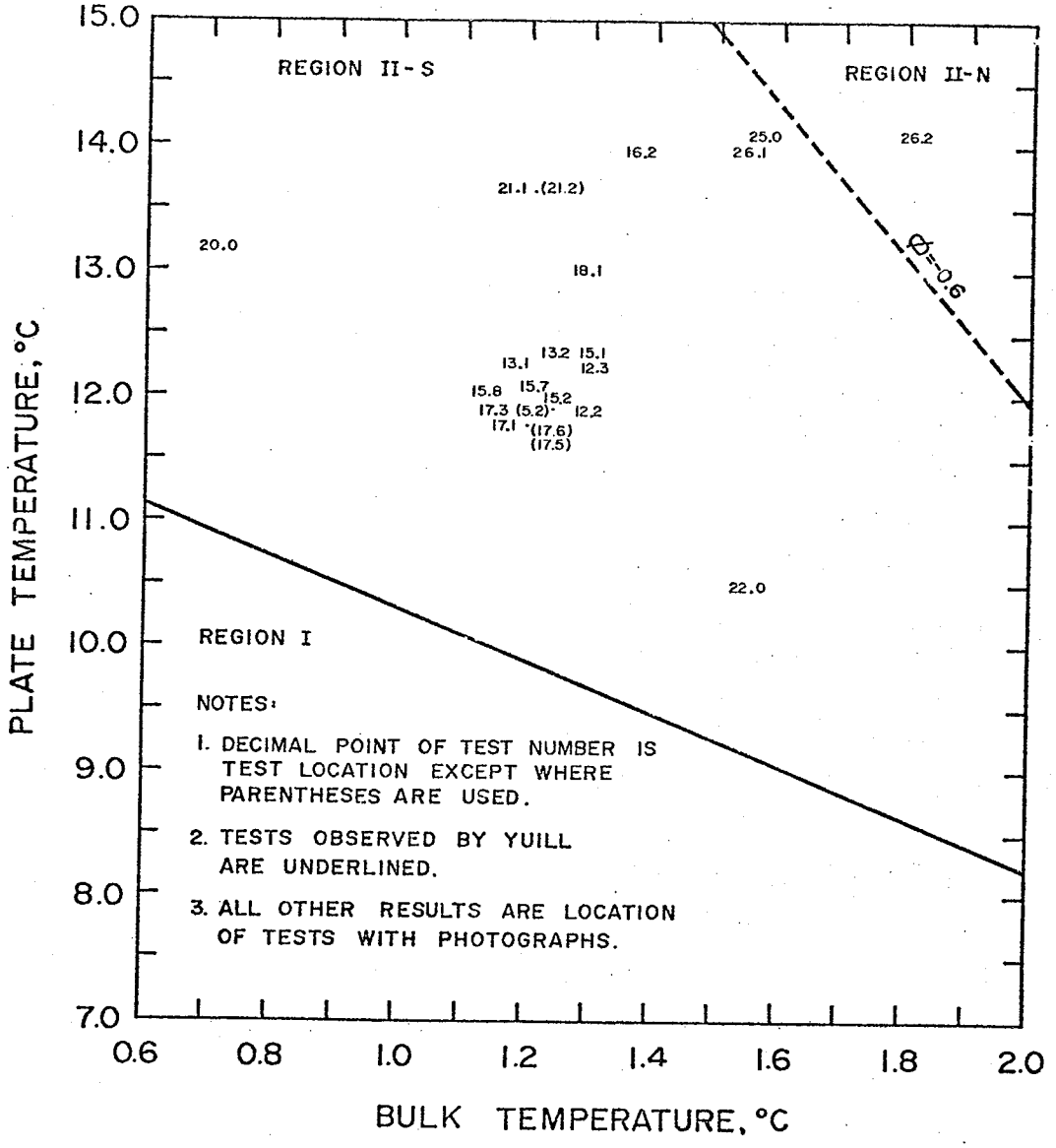

FIGURE 12 REGION II FLOW VISUALIZATION TESTS

TABLE IV

FLOW VISUALIZATION TESTS

TEST NO.	PROBE LOCATION	PROBE TYPE	PHOTOGRAPH INTERVAL, SEC.
5.2	midpoint	beaded	3
12.2	top	bare	5
12.3	top	bare	5
13.1	top	bare	5
13.2	top	bare	5
15.1	top	bare	5
15.2	midpoint	bare	5
15.7	midpoint	beaded	3
15.8	midpoint	beaded	3
16.2	midpoint	beaded	3
17.1	midpoint	beaded	3
17.3	midpoint	beaded	3
17.5	midpoint	beaded	3
17.6	midpoint	beaded	3
18.1	midpoint	beaded	3
20.0	midpoint	beaded	3
21.1	midpoint	beaded	3
21.2	midpoint	beaded	3
22.0	midpoint	beaded	3
25.0	top	bare	no photos
26.1	top	bare	no photos
26.2	top	bare	no photos

Test 15.2. In these tests the photographic quality ranged from fair to good. The interval between photographs for all tests except 15.2 was 3 seconds. For 15.2 it was 5 seconds. The contrast and definition were not as good as for the other photographs.

In Figure 12 it can be seen that all of the flow visualization results except Test 26.2 lie in the region designated by Yuill (1) as the "separated" bidirectional flow region, Region II-S. Test 26.2 lies in the "non-separated" bidirectional flow region. The flow patterns observed are discussed in the following section.

3.2.2 Examination of Flow Patterns

In the Region II-S tests with the probe at the top of the heated section the inner boundary layer could be seen to rise up above the heated section, separate from the plate and reverse its flow direction to return as the outer boundary layer.

In the discussion that follows one set of test photographs will be discussed in frame by frame sequence and the highlights or significant features of individual tests will be discussed briefly. The photographic negatives for all tests are on file in the Department of Mechanical Engineering at the University of Manitoba.

The photographs from Test 15.1 are presented in the

following pages as Figures 13(a) to 13(j). The bare wire probe that produces a continuous sheet of dye was used in this test. It was located at the top of the heated section. The photographs were taken at 5 second intervals, starting 5 seconds after production of the dye.

In the second photograph flow both above and below the heated section is evident. However, in this photograph and in those following the flow only proceeds about 5 mm up past the top of the heated section and then separates from the plate.

The advancing point of the dye front begins to sweep closer to the plate in Figures 13(b) to 13(d) and then proceeds down the plate at a distance of approximately 7.0 to 7.5 mm from the plate. In Figures 13(f) and 13(g) a streak of dye begins to trace out an upward flow in the inner boundary layer. In Figures 13(g) to 13(i) a faint dye streak can be seen to flow up past the top of the heated surface and return in the outer boundary layer. There appears to be a cell of complete recirculation within the boundary layer.

In Tests 12.2 and 12.3 the dye initially streams up off the wire. The probable cause is the formation of hydrogen bubbles on the wire due to too high a potential on the wire or too long a duration of the potential.

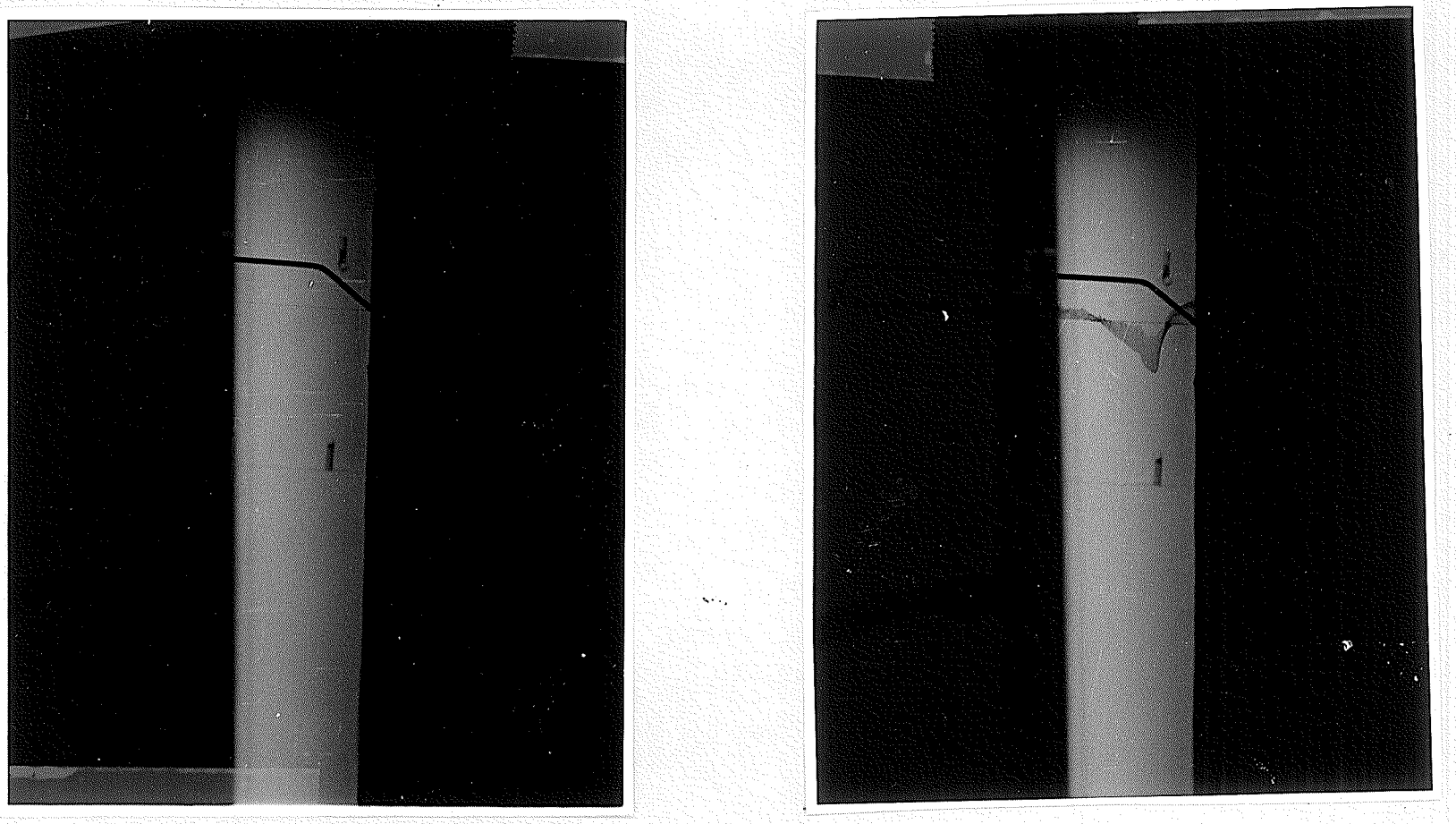

(a) (b)

FIGURE 13 TEST 15.1 FLOW VISUALIZATION PHOTOGRAPHS

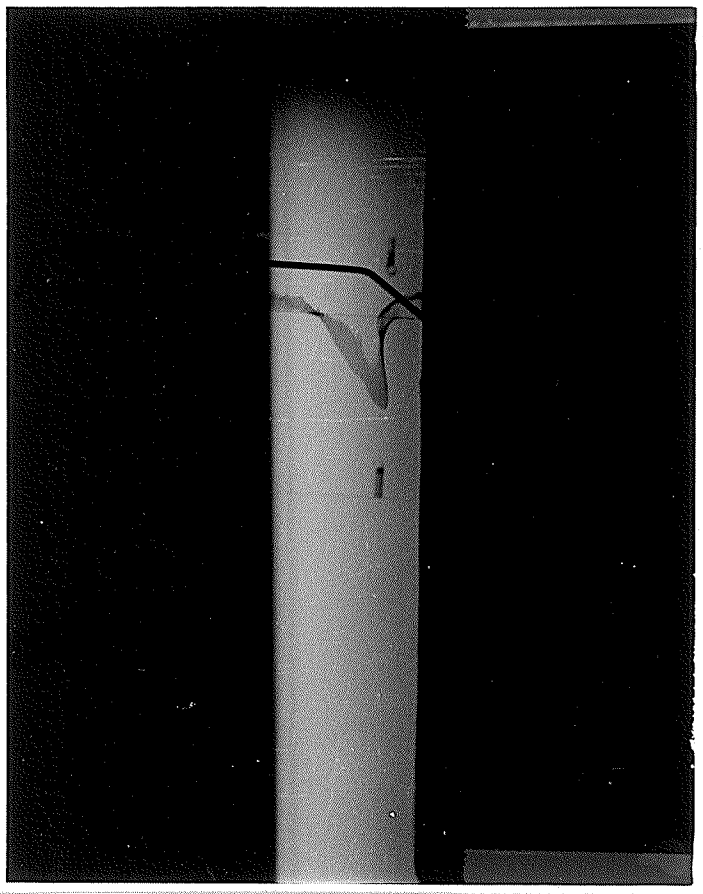

(c)

(d)

FIGURE 13 (CONTINUED)

(e)

(f)

FIGURE 13 (CONTINUED)

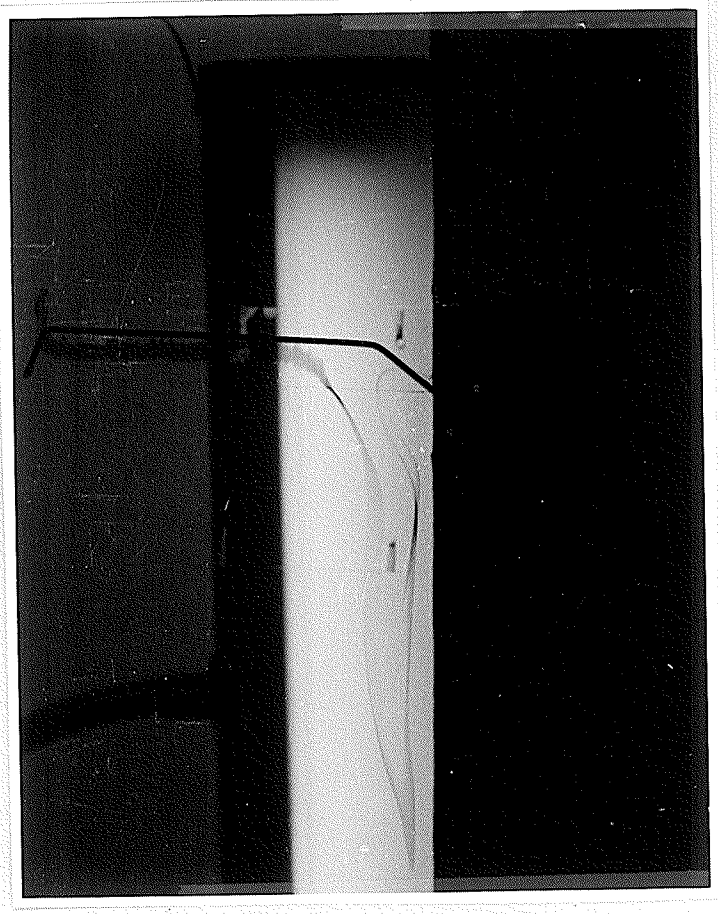

(g)

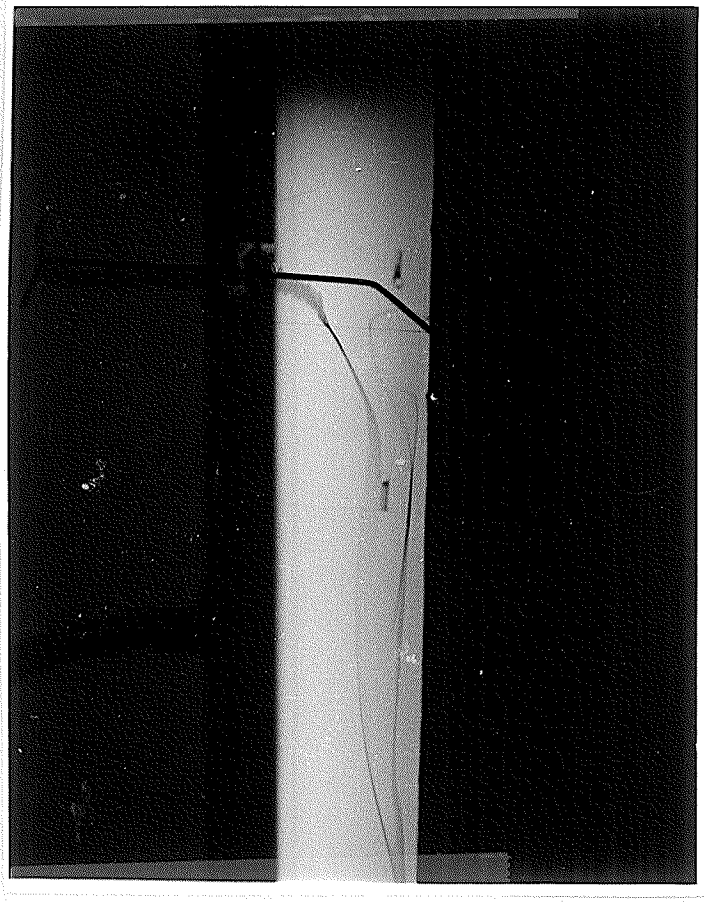

(h)

FIGURE 13 (CONTINUED)

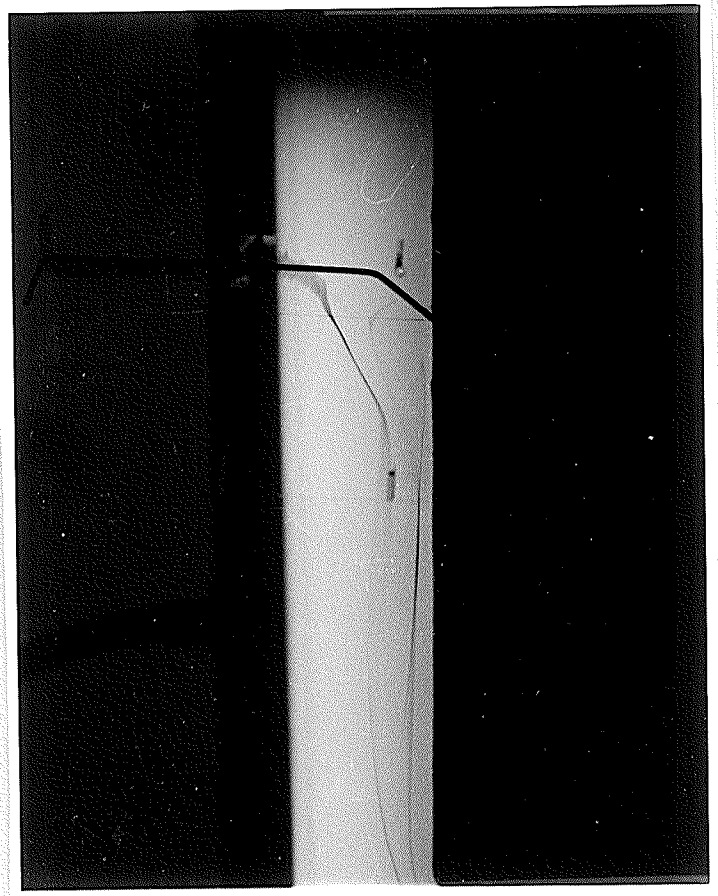

(i)

(j)

FIGURE 13 (CONTINUED)

Separation of the flow above the heated section is evident. The dye also traces out a cell of complete recirculation at the top of the heated section. Viscous forces in the outer downward flowing boundary layer appear to pull dye down from the bottom of the circulation cell.

The dye that is visible travelling up from the wire at a distance away from the plate and also up the plate surface is due to the bubble formation on the wire. The results from Test 12.3 are very similar to those of 12.2.

In Test 13.1 there is no evidence of bidirectional flow. A check of the raw experimental data showed that the photographs were taken 30 minutes after the start of the test. It appears that the flow had not fully developed since Test 13.1 is well within the bidirectional flow region. The flow visible in the photographs is that of purely downward flow. The advancing dye front traces out the usual free convective velocity profile.

Test 13.2 was run at almost exactly the same bulk and plate temperatures as 13.1. The photographs were taken one hour after the beginning of the test. They show an outer boundary layer very similar to Test 13.1. However, the inner boundary layer separates above the top of the heated section and some recirculation is evident. The extent of the recirculation is not as great

as in Test 15.1.

For Test 15.2 the probe was positioned at the midpoint of the heated section. The contrast in this set of photographs is very poor and it is difficult to see the flow patterns. The downward flowing outer boundary layer can be seen. It is difficult to see inner upward flow because of the faintness of the dye trace. Some flow above the wire is evident.

The above photographs were all taken by the author. At the time of completion of the above tests both the test procedure and photographic technique had been established and proven and all that was necessary to complete the testing was to repeat the procedure at various points throughout Regions II-S and II-N.

The above photographs provided qualitative results. It was difficult to determine flow velocities or other quantitative results from the sheet of dye produced by the bare wire probe. A suggestion was made to try a probe in which streaks of dye could be produced.

The research assistants used a beaded probe in all of the remaining tests. Also, in the balance of the tests the probe was located at the midpoint. The assistants used a slightly different procedure than the author. They attempted various combinations of camera lenses, shutter

speeds, and aperture settings. The photographic results obtained in this fashion are of poor quality and it is difficult to gain a detailed understanding of the flow phenomena from them. However, the highlights of the photographs are discussed below.

Only the downward flowing boundary layer is visible in the photographs from Test 5.2. In the photographs from Test 15.7 a faint trace of upward flow from the wire can be detected. It appears that either the probe is interfering with the flow or the wire has been insulated too close to the plate surface. There is also a fair amount of streaming of dye off the wire immediately after formation of the dye. The photographs from Test 15.8 do not have sufficient contrast to permit examination.

Upflow in the inner boundary layer is visible in the first few frames of the photographs for Test 16.2. The inner boundary layer flow, however, is faint. There is not enough dye produced immediately adjacent to the plate.

A faint upflow, similar to that observed in Test 16.2, is evident in the first few photographs from Tests 17.3 and 17.5.

For Test 17.6 the lighting arrangement was changed from a single flourescent tube to a bank of tubes. The photographs were taken with a telephoto lens at various

aperture settings with a series of four photographs for each dye trace. The outer boundary layer is visible but the inner flow can not be seen at all.

In Test 18.1 both the inner and outer boundary layers are visible and there is no question about the existence of two distinct flow directions. There appears to be a general upflow in the bulk fluid as indicated by dye traces at a distance from the plate. As there was no appreciable change in the bulk fluid temperature over the period of the test, the upflow of dye must be due to bubble formation on the wire or local heat fluxes produced by the probe wire.

The first four photographs for Test 20.0 illustrate both the inner and outer boundary layer flows. However, the dye produced close to the plate is not dense enough to be visible in the later photographs. Again there is little dye produced immediately adjacent to the plate.

Two dye traces are visible in Test 21.1 photographs. In the first four pictures, taken at 3 second intervals the inner boundary layer is only faintly visible. In the second set the inner boundary layer can be seen to rise above the probe. The width of the inner boundary layer at the probe height is approximately 4.5 mm. The dye traces in Test 21.2 are too faint to be examined.

For Test 22.0 three dye traces were produced at 12 second intervals. Photographs were taken at 3 second intervals. However, the dye traces are faint and although both inner and outer boundary layers can be seen to exist, little else can be gained from an examination of the photographs.

No photographs were obtained of the last three tests; 25.0, 26.1 and 26.2. The flows were observed and the descriptions are given below.

In Test 25.0 separation at the top of the heated section was seen. There was no flow up the plate above the heaters. In Test 26.1 circulation was observed. There appeared to be recirculation and separation at the top of the plate, but much less than usual. The dye continued up the plate about 20 mm then separated and circulated down on a 10 mm radius.

In Test 26.2 the inner flow went right up the plate to the top. Some later recirculation was evident at the top of the heated section but it was not significant.

3.2.3 Boundary Layer Measurements

Inner and outer boundary layer widths were scaled from the photographs. The results are given in Table V and are divided into two cases;

a) probe at the top of the heated section, and

TABLE V

BOUNDARY LAYER DIMENSIONS

(a) Probe at Top of Heated Section.

Test No.	Outer Bound. Layer at Wire, mm	Inner Bound. Layer at Wire		Range of Width of Inner Bound. Layer, mm
		Downflow Region, mm	Upflow Region, mm	
12.3	34.0	13.0	4.0	6.0 to 4.0
13.1	34.0	-	-	2.0
13.2	34.0	4.0	negligible	2.0
15.1	29.0	17.0	2.0	7.0 to 1.7

(b) Probe at Midpoint of Heated Section.

Test No.	Bound. Layer Width at Wire		Range of Width of Inner Bound. Layer, mm	Height Visible Above Wire, mm
	Outer, mm	Inner, mm		
15.7	23.0	4.5	4.5-1.5	-
17.3	16.0	3.0	3.0	-
18.1	32.0	3.0	1.7-3.0-5.0	17.0
20.0	21.0	4.5	3.0-4.5-3.0	-
21.1	30.0	4.5	4.5-6.0	-
22.0	20.0	4.5	4.5-3.0	-

b) probe at the midpoint of the heated section.

The outer boundary layer widths for Tests 12.2, 12.3, 13.1, 13.2 and 15.1 ranged from 34 to 29 mm at the top of the heated section. In those tests in which recirculation was evident, Tests 12.2, 12.3, 13.2 and 15.1, the downward flowing outer section of the recirculation cell ranged from 4 mm in Test 13.2 to 17 mm in Test 15.1 from the plate surface. The width of the inner upward flowing boundary layer at the top of the heated section was approximately 2 mm in Test 15.1, 4 mm in Test 12.3 and negligible in Test 13.2. In Test 13.1 there was no visible inner up flowing boundary layer at the wire. The range in width of the inner boundary along the plate height is also given. In Test 12.3 the width ranged from 4 mm at the wire to 6 mm further down the plate. In Test 15.1 the width ranged from 1.7 mm at the wire to 7 mm at the bottom of the heated section.

For tests with the probe at the midpoint of the heated section the outer boundary layer width at the wire ranged from 16 mm to 32 mm. The inner boundary layer width at the wire ranged from 3 mm to 4.5 mm. The range of the boundary layer widths over the plate height is also given. The width range above includes cases in which flow above the wire was visible. In Test 18.1

the dye was visible to a height of 17 mm above the wire.

Dye front velocities were also scaled from the photographs. It was not possible to obtain discrete point velocities from the dye traces. Velocity vectors could not be determined. However, the general movement of the "peak" of the dye trace was examined and the speed of the dye fronts calculated. In Tests 12.3 and 15.1, with the probe at the top of the 15.24 cm heated plate, the dye trace appeared to accelerate towards the bottom of the plate. The speed of the dye trace varied from 2 mm/sec over the first 15 mm to 8.5 mm/sec over the bottom 30 mm of the plate.

In Tests 13.1 and 13.2 the speed of the dye trace was fairly constant over the plate height and averaged 2.5 mm/sec in Test 13.1 and 2.3 mm/sec in Test 13.2.

In tests with the probe at the midpoint of the heated section the speed of the outer boundary layer dye trace varied from 1.8 mm/sec in Test 17.3 to 6.3 mm/sec in Test 21.1. In Test 18.1 it was possible to calculate the average speed of the upward flowing inner boundary layer. The speed was 1.2 mm/sec.

Schechter (13) reported the results of boundary layer velocity measurements for only two tests in the bidirectional flow region. However, the test locations were not

close to those in the present investigation. The order of magnitude of the velocities reported are in agreement with the dye front speeds recorded in the present investigation. The two tests reported were conducted at bulk temperatures of 2.97°C and 3.22°C and plate temperatures of 8.1°C and 8.96°C respectively. In the test at a bulk temperature of 3.22°C and plate temperature of 8.96°C the velocity in the outer boundary layer was given as 3.8 mm/sec. In the same test the velocity in the upward flowing inner boundary layer was reported to be 1.5 mm/sec. The patterns observed are also similar to those reported in this investigation. The inner and outer boundary layer velocities in the other test are given as 1.2 mm/sec. and 1.8 mm/sec.

3.2.4 Comparison of Flow Visualization with Yuill's Hypothesis

A description of the flow patterns predicted by Yuill in the bidirectional flow region is given in section 2.1 of this report. As reported in section 3.1.3 of this report the test results in Region II can be separated into two distinct regions in accordance with the percentage change of temperature from the last heated section to the first unheated section.

Test 26.2 falls into the region designated by Yuill (1)

as "non-separated" flow. One would expect the inner boundary layer flow to continue up past the top of the heated section if Yuill's hypothesis is true. Observations of the dye flow in this test indicated that the inner boundary layer flow proceeded up past the top of the heated section to the top of the plate.

The other flow visualization test results lie in the region designated by Yuill as "separated" flow. Photographs of the dye traces and visual observations confirm that the inner boundary layer separates from the plate at the top of the heated section and flows back down in the outer boundary layer. In some photographs a recirculation cell is evident at the top of the heated section.

CHAPTER 4

CONCLUSIONS

The major objective of this work was to investigate the boundary layer flows and heat transfer that exist in free convective heat transfer from a vertical isothermal plate to water below $4^{o}C$ in a region in which bidirectional flow is known to exist. Experimental correlations developed in an earlier investigation (1) were to be tested against experimental results obtained using a different apparatus.

It was shown that Yuill's experimental correlations predicted mean fluxes that ranged from -9.28% to +18.31% from the present experimental results. The magnitude of the error was shown to be a function of the correlating variables suggesting that additional data must be collected in order to improve upon the form of the correlation.

The flow visualization studies performed indicated that two types of bidirectional flow patterns exist. In "separated" bidirectional flow the inner upward flowing boundary layer was observed to flow up just above the heated section of the plate, separate from the plate and flow back down into the outer downward flowing boundary layer. A cell of complete recirculation of flow was visible within the boundary layer. In "non-separated"

flow, the inner boundary layer was observed to continue flowing up past the top of the heated section of the plate to the top of the unheated section. With only one test in this region it was impossible to predict the boundary of the "separated" and "non-separated" flow regions. Additional flow visualization tests are required to establish the boundaries between the regions.

The "thymol blue" flow visualization technique proved to be more suitable for qualitative studies than for quantitative studies. Boundary layer widths were scaled from photographs and the dye front speeds were calculated. These results are reported in section 3.2.3 of this report.

Future investigations in this area of free convective heat transfer should be directed towards obtaining additional information concerning the nature of the flow patterns in the vicinity of the heated plate surface at various heights. The flow phenomena would be better understood if it were possible to generate dye traces immediately adjacent to the plate surface.

REFERENCES

1. G. K. Yuill, "Free Convective Heat Transfer From a Vertical Isothermal Plate to Water Near 4°C", Ph. D. thesis, U. of Minn., (1972).

2. C. R. Vanier, "Free Convective Melting of Ice", M.S. thesis, Syracuse Univ., N.Y., (1968).

3. L. Lorenz, "Ueber das Leitsvermogen der Metalle fur Warme und Electricitat", Wiedemanns Annalen, 13, 582, (1881).

4. E. Schmidt, and W. Beckman, "Das Temperatur-und Geshwindigketsfeld vor einter Warme abgebenden senkrechter Platte bei naturlicher Konvektion", Tech. Mech. u. Thermodynamik, 1, No. 10, p. 341, (1930).

5. E. Polhausen, Tech. Mech. u. Thermodynamik, 1, No. 11, p. 391, (1930).

6. C. Codegone, "Su un punto d'inversione die moti convettive", Acc. Sci. Torino Atti, 75, p. 167, (1939).

7. A. J. Ede, "Heat Transfer by Natural Convection in Refrigerated Liquids", Eighth Int. Cong. Refrig., p. 260, London, 1951.

8. A. G. Tkachev, "Heat Exchange in Freezing and Melting of Ice", Problems of Heat Transfer During a Change of State, AEC-Tr-3405, Translated from a Publication of the State Power Press, Moscow Leningrad, p. 169, (1953).

9. J. M. Dumore, H. J. Merk and J. O. Prins, "Heat Transfer from Water to Ice by Thermal Convection", Nature, 172, p. 460, (1953).

10. H. J. Merk, "The Influence of Melting and Anomalous Expansion on the Thermal Convection In Laminar Boundary Layers", Appl. Sci. Res. A4, p. 435, (1954).

11. A. J. Ede, "The Influence of Anomalous Expansion on Natural Convection in Water", Appl. Sci Res., A5, p. 458, (1955).

12. R. S. Schechter, and H. S. Isbin, "Natural Convection Heat Transfer in Regions of Maximum Fluid Density", JAIChE, 4, p. 81, (1958).

13. R. S. Schechter, "Natural Convection Heat Transfer in Regions of Maximum Fluid Density", Ph. D. thesis, U. of Minn., (1956).

14. S. Ostrach, "An Analysis of Laminar Free Convection Flow and Heat Transfer About a Flat Plate Parallel to the Direction of the Generating Body Force", NACA Report No. 1111, (1953).

15. S. L. Goren, "On Free Convection in Water at $4^{o}C$", Chem. Eng. Sci., 21, p. 515, (1966).

16. C. A. Oborin, "Special Features of Free Convection at Temperatures Below $277^{o}K$", Journal of Eng. Phys., 13, No. 6, p. 837, (1967).

17. J. Schenk, and F.A.M. Schenkels, "Thermal Free Convection from an Ice Sphere in Water", Appl. Sci. Res., 19, p. 465, (1968).

18. C. R. Vanier, "Free Convection Melting of Ice Spheres", JAIChE, 16, p. 76, (1970).

19. C. R. Vanier, and C. Tien, Letter to the Editors, Appl. Sci. Res., 21, p. 387, (1969).

20. C. R. Vanier, and C. Tien, "Further Work on Free Convection at $4^{o}C$", Chem. Eng. Sci., 22, p. 1747, (1967).

21 C. R. Vanier, and C. Tien, "Effect of Maximum Density and Melting on Natural Convection Heat Transfer from a Vertical Plate", Chem. Eng. Prog. Symp. Series, 64, p. 240, (1968).

22. D. J. Baker, "A Technique for the Precise Measurement of Small Fluid Velocities", J. Fluid Mech., 26, p. 573, (1966).

23. E. M. Sparrow, and R. B. Husar, "Longitudinal Vortices in Natural Convection Flow on Inclined Plates", J. Fluid Mech., 37, p. 251, (1969).

24. J. R. Lloyd, and E. M. Sparrow, "On the Stability of Natural Convection Flow on Inclined Plates", J. Fluid Mech., 42, p. 465, (1970).

APPENDIX I

VARIATION OF HEATER RESISTANCE WITH TEMPERATURE

The main and guard heater resistances were calibrated as a function of plate temperature. The resistances were evaluated at a minimum plate temperature of $5^{o}C$ and a maximum temperature of $18^{o}C$. The heater resistance at any temperature between these extremes was evaluated by assuming a linear variation of heater resistance with temperature. A straight line equation of the form

$$R_T(i) = R_5(i) + S(i) \times (T-5.0)$$

was used. The values of $R_5(i)$ and $S(i)$ for the main and guard heaters are given in Table I-A.

TABLE I-A

VARIATION OF HEATER RESISTANCE

MAIN HEATERS

HEATER NO.	$R_5(i)$	S(i)
1	3.536	.00131
2	3.462	.00092
3	3.3600	.00089
4	3.3785	.00065
5	3.534	.00913
6	3.551	.00131
7	3.546	.00131
8	3.543	.00131
9	3.568	.00138
10	3.531	.00169

GUARD HEATERS

HEATER NO.	$R_5(i)$	S(i)
1	3.588	.001
2	3.5736	.00086
3	3.4949	.00083
4	3.5432	.00084
5	3.5213	.00078
6	3.6091	.00093
7	3.6149	.00092
8	3.6236	.00115
9	3.5667	.00135
10	3.5874	.00162

APPENDIX II

DECAY OF TEMPERATURE ALONG THE ADIABATIC SECTION

In the six heater tests in Region II the plate temperatures above the heated section were recorded. The decay of temperature along the adiabatic section was examined by considering the slope of the temperature gradient from the last heated section to the first unheated section. Thus if T_i is the temperature of the last heated section, T_{i+1} is the temperature of the first unheated section, and θ_p is the difference between the plate temperature and bulk temperature, then S_i, the temperature gradient is given by:

$$S_i = \frac{T_i - T_{i+1}}{\theta_p} \times 100.$$

The values of S_i for the six heater tests are tabulated in Table II-A.

TABLE II-A

COMPARISON OF TEMPERATURE OF LAST HEATED SECTION & FIRST UNHEATED SECTION

TEST NO.	BULK TEMP.	PLATE TEMP.	$\frac{\Delta T}{\theta_p}$, %
4.0	1.91	9.97	74.434
5.1	1.28	11.84	75.486
5.2	1.24	11.90	77.813
6.0	1.38	12.87	73.131
12.1	1.29	12.01	76.599
12.2	1.30	11.85	79.823
12.3	1.31	12.20	78.736
13.1	1.19	22.22	80.316
13.2	1.25	12.31	80.187
14.0	1.04	13.15	77.859
15.1	1.31	12.31	-
15.2	1.25	11.95	78.827
15.3	1.27	12.07	79.632
15.4	1.25	11.81	80.565
15.5	1.25	12.02	79.093
15.6	1.23	11.48	80.826
15.7	1.22	12.03	79.536
15.8	1.14	12.00	79.290
16.1	1.51	13.82	70.199
16.2	1.38	13.93	69.029
17.1	1.17	11.74	80.152
17.2	1.14	11.46	79.704
17.3	1.15	11.85	80.235
17.4	1.17	11.79	80.453
17.5	1.20	11.78	80.129
17.6	1.20	11.79	80.502
18.1	1.30	12.97	74.996
18.2	1.25	12.86	75.670
19.0	1.57	10.11	77.634
20.0	0.72	13.13	79.757
21.1	1.18	13.63	76.078
21.2	1.21	13.63	74.843
21.3	1.26	13.76	74.176
22.0	1.56	10.45	79.382
23.1	.66	12.88	82.099
24.0	.67	11.84	79.458
25.0	1.58	14.06	-
26.1	1.56	13.94	67.483
26.2	1.82	14.07	33.336